RESEARCH ARTICLE

Prokaryotic community structure and diversity in the sediments of an active submarine mud volcano (Kazan mud volcano, East Mediterranean Sea)

Maria G. Pachiadaki[1,2], Vasilios Lykousis[2], Euripides G. Stefanou[1] & Konstantinos A. Kormas[3]

[1]Environmental Chemical Processes Laboratory, Department of Chemistry, University of Crete, Voutes-Heraklion, Greece; [2]Hellenic Centre for Marine Research, Institute of Oceanography, Anavissos, Greece; and [3]Department of Ichthyology and Aquatic Environment, School of Agricultural Sciences, University of Thessaly, Nea Ionia, Greece

Correspondence: Konstantinos A. Kormas, Department of Ichthyology and Aquatic Environment, School of Agricultural Sciences, University of Thessaly, 384 46 Nea Ionia, Greece. Tel.: +30 242 109 3082; fax: +30 242 109 3157; e-mail: kkormas@uth.gr

Received 12 October 2009; revised 24 January 2010; accepted 9 February 2010.
Final version published online 29 March 2010.

DOI:10.1111/j.1574-6941.2010.00857.x

Editor: Riks Laanbroek

Keywords
Bacteria; *Archaea*; 16S rRNA gene; diversity; Kazan marine mud volcano.

Abstract

We investigated 16S rRNA gene diversity at a high sediment depth resolution (every 5 cm, top 30 cm) in an active site of the Kazan mud volcano, East Mediterranean Sea. A total of 242 archaeal and 374 bacterial clones were analysed, which were attributed to 38 and 205 unique phylotypes, respectively (≥98% similarity). Most of the archaeal phylotypes were related to ANME-1, -2 and -3 members originating from habitats where anaerobic oxidation of methane (AOM) occurs, although they occurred in sediment layers with no apparent AOM (below the sulphate depletion depth). *Proteobacteria* were the most abundant and diverse bacterial group, with the *Gammaproteobacteria* dominating in most sediment layers and these were related to phylotypes involved in methane cycling. The *Deltaproteobacteria* included several of the sulphate-reducers related to AOM. The rest of the bacterial phylotypes belonged to 15 known phyla and three unaffiliated groups, with representatives from similar habitats. Diversity index *H* was in the range 0.56–1.73 and 1.47–3.82 for *Archaea* and *Bacteria*, respectively, revealing different depth patterns for the two groups. At 15 and 20 cm below the sea floor, the prokaryotic communities were highly similar, hosting AOM-specific *Archaea* and *Bacteria*. Our study revealed different dominant phyla in proximate sediment layers.

Introduction

Mud volcanoes (MVs) result from the extrusion of fluid-rich mud flows and have long been known onshore and at sea, mainly within active tectonic belts, but also on passive margins with high sedimentation rates. Submarine MVs have become environments of intensive study in recent years. They play an intrinsic role in many processes such as the shaping of ocean margins, release of greenhouse gases and thus climate change, petroleum genesis and accumulation of gas hydrates, a potential energy resource (Milkov, 2000). MVs may erupt violently at regular or irregular time intervals or may emit mud, fluid and gases continuously. In the eastern Mediterranean Sea, MVs and seep areas were discovered during the late 1970s (Cita *et al.*, 1981) and continuing research has revealed several such formations on the accretionary prism of the Hellenic Arc (Mediterranean Ridge) and within the Anaximander Mountains (Woodside *et al.*, 1998; Lykousis *et al.*, 2004). Kazan MV is an isolated, oval-shaped 0.6 × 0.9 km dome aligned in a N–S direction, with a height of 50 m, lying on the edge of a relatively flat plateau of 1750 m average depth (Lykousis *et al.*, 2009); it has been regarded as rather inactive.

High seafloor methane fluxes are associated with MVs as well as with the accompanying cold vents and seeps (Charlou *et al.*, 2003). The available gas provides energy for rich benthic communities, which include chemosynthetic symbiotic fauna (Olu-Le Roy *et al.*, 2004). Moreover, highly diverse and productive microbial ecosystems based on chemosynthesis can be sustained by the carbon-rich fluids in MVs. Probably the most important biogeochemical process fuelling these communities at these locations is the anaerobic oxidation of methane (AOM) (Boetius & Suess, 2004). In marine habitats, the metabolic process of AOM is

suggested to be a reversed methanogenesis coupled to the reduction of sulphate-involving methanotrophic archaea (ANME archaea) and sulphate-reducing bacteria (SRB) (Hallam *et al.*, 2004).

Studies have provided evidence for the occurrence of AOM in Kazan carbonate crusts, based on carbon isotopic signatures, porewater chemistry and general molecular fingerprints (Aloisi *et al.*, 2000; Werne *et al.*, 2002; Boulouba ssi *et al.*, 2006; Heijs *et al.*, 2006), as well as in specific sediment layers of the Kazan MV (Werne *et al.*, 2004; Heijs *et al.*, 2007; Kormas *et al.*, 2008).

There is a scarcity of available data on the fine-scale distribution of prokaryotes in marine surface sediments. However, the co-occurrence patterns of microorganisms are the first step in defining potentially interacting organisms and interaction networks in highly complex systems and also help to define ecological niches for better characterization of ecological species or microbial ecotypes. In addition, the relationship between co-occurring communities with environmental factors helps to delineate species that are specific to such sediments (Fuhrman, 2009).

The structure of highly complex prokaryotic communities in marine sediments is dictated by rapid changes of physical and geochemical factors with sediment depth in hot-spot sites such as MVs. However, it remains unclear whether such factors shape the communities of *Bacteria* and *Archaea* in a similar manner. Here, we investigated whether: (1) the community structures of *Bacteria* and *Archaea* vary concomitantly; (2) the prokaryotic assemblages are dominated by one or several phylotypes with different relative abundances, implying a specific or an opportunistic community, respectively; and (3) which of these specific communities are involved in biogeochemical processes related to mud volcanism. We analysed the diversity of *Archaea* and *Bacteria* every 5 cm in the top 30 cm of sediment in an active site of the Kazan MV, East Mediterranean Sea.

Materials and methods

Sampling site

The data presented in this study were acquired from the Kazan MV in May 2003. Selected seismic reflection profiling and sediment sampling were carried out in order to better evaluate the most active sites bearing gas hydrates. The seafloor bathymetry/backscatter survey was carried out using a SEABEAM 2120 swath system installed aboard the R/V *AEGAEO* of the Hellenic Centre for Marine Research (see fig. 10 in Lykousis *et al.*, 2009). The backscattered multibeam (backscattering intensity) map of the Kazan MV revealed a clear tail-like structure, prominently directed towards the south, suggesting the presence of a mud flow. The highest backscatter values corresponded to the summit of the mound, which was expected to be the more active site of the MV, while concentric to this, the backscatter variations seemed to correspond to variations in the slope of the volcano. Gas hydrates were recovered for the first time at Kazan MV during the cruise reported in this paper. The gas hydrate crystals appeared as small rice-like lumps and were quite regularly dispersed throughout the sediment matrix, even close to the sediment surface (inset to fig. 11 in Lykousis *et al.*, 2009).

Gas-hydrate-containing sediment samples were collected from a site (35°25′55″N, 30°33′42″E) of the Kazan MV, where mud flow indicated recent activity, as described in Kormas *et al.* (2008). Prokaryotic diversity at 1, 5, 10, 25 and 30 cm below the sea floor (cm b.s.f.) was analysed. Data from 15 and 20 cm b.s.f. were retrieved from the same sediment core and are taken from Kormas *et al.* (2008).

DNA extraction, amplification and cloning

DNA was extracted from 1 g of wet sediment from each sample, using the UltraClean Soil DNA kit (MoBio Laboratories Inc.) following the manufacturer's protocol with minor modifications: bead beating was reduced from 10 to 5 min, and this step was immediately followed by three freeze–thaw cycles (− 80 °C for 3 min and then immediately in a 65 °C water bath for 5 min) after addition of the inhibitor removal solution. Bacterial 16S rRNA genes were amplified using the bacterial primers B8f–B1492r (Teske *et al.*, 2002). The PCR included an initial denaturation step at 94 °C for 1 min, followed by 27–31 cycles consisting of denaturation at 94 °C for 45 s, annealing at 52.5 °C for 45 s and elongation at 72 °C for 2 min; a final 7-min elongation step at 72 °C was added. The archaeal 16S rRNA gene was amplified using the primer combination A8f and A1492r (Teske *et al.*, 2002). An initial denaturation step at 94 °C for 1 min was followed by 25–29 cycles consisting of denaturation at 94 °C for 45 s, annealing at 52.5 °C for 45 s and elongation at 72 °C for 2 min; a final 7-min elongation step at 72 °C was added. The number of cycles was determined for each sample after cycle optimization. PCRs were repeated with different cycle numbers, and the lowest number of cycles that yielded a positive signal was then used for cloning and sequencing in order to avoid differential representation of 16S rRNA genes with low and high copy numbers (Spiegelman *et al.*, 2005). Eight tubes of PCR products were pooled for cleanup and cloning to reduce the bias of each individual reaction.

PCR products were visualized on a 1% agarose gel under UV light, bands were excised and PCR products were extracted using the Wizard SV Gel and PCR Clean-up kit (Promega Inc.) following the manufacturer's protocol. The PCR products were cloned using the TOPO TA Cloning® Kit for Sequencing (Invitrogen Corp.) using

electrocompetent cells according to the manufacturer's specifications. For each sample and each gene, randomly picked clones with inserts of the expected length were analysed. Clones were grown in liquid Luria–Bertani medium with kanamycin and their plasmids were purified using the NucleoSpin Plasmid QuickPure kit (Macherey-Nagel GmbH & Co. KG, Germany) for DNA sequencing.

Sequencing and phylogenetic analysis

Sequence data were obtained by Macrogen Inc. (South Korea) using capillary electrophoresis and a BigDye Terminator kit (Applied Biosystems Inc.) with the primers M13F(-20) and M13R. Every sequence read was approximately 900 bp, and for each individual clone, forward and reverse reads were assembled. The sequences were screened for chimeras by comparing neighbour-joining trees made of the first and second halves of all sequences. The sequences that had different groupings in the first and second halves were then checked using the PINTAIL program (Ashelford *et al.*, 2005; http://www.bioinformatics-toolkit.org/Web-Pintail/). BELLEROPHON software from GreenGene (DeSantis *et al.*, 2006) (http://greengenes.lbl.gov/cgi-bin/nph-bel3_interface.cgi) was also used to detect chimeric sequences. All putative chimeras were excluded from further analysis.

For the detection of the closest relatives, all sequences were compared with the BLAST function (Zhang *et al.*, 2000; http://www.ncbi.nlm.nih.gov/BLAST/). The sequences were automatically aligned against sequences from their closest relatives using the RDP alignment utility (Cole *et al.*, 2003; https://rdp.cme.msu.edu/) and revised by manual removal of ambiguously aligned regions. Phylotypes or operational taxonomic units were defined as sequences showing $\geq 98\%$ homology (Fields *et al.*, 2006) to each other.

Phylogenetic trees were constructed by the neighbour-joining method using the Kimura two-parameter correction. Bootstrap analyses for 1000 replicates were performed to assign confidence levels to the tree topology using the MEGA4 software (Tamura *et al.*, 2007). Sequences of unique phylotypes found in this study have GenBank numbers FJ712361–FJ712398 for *Archaea* and FJ712399–FJ712411, FJ712413–FJ712428, FJ712432–FJ712451, FJ712453–FJ712462, FJ712466–FJ712472, FJ712478–FJ712483, FJ712489–FJ712509, FJ712511–FJ712514, FJ712516–FJ712536, FJ712538–FJ712555, FJ712557–FJ712560, FJ712562–FJ712568 and FJ712570–FJ712621 for *Bacteria*.

Clone library coverage, diversity and similarity analyses

Clone coverage was calculated using the equation $C = [1 - (n_i/N)] \times 100$, where n_i is the number of phylotypes and N is the number of 16S rRNA gene sequences examined (Good, 1953; Kemp & Aller, 2004). The Shannon–Wiener index H was used as a diversity index and was calculated as follows: $H = -\sum p_i \cdot \ln p_i$, where the summation is over all phylotypes i and p_i is the proportion of phylotypes relative to the sum of all phylotypes. The Pielou evenness index J was calculated as $J = H/\ln S$, where S is the total number of phylotypes (Shannon & Weaver, 1949; Pielou, 1969).

The similarity among the microbial communities in all sediment layers was determined using the Morisita index of similarity (Wolda, 1981) at both the phylotype and the phylogenetic group level, using the equation

$$\text{Morisita}_{jk} = \frac{2\sum_{i=1}^{S}(n_{ij}n_{ik})}{(\lambda_1 + \lambda_2)\sum_{i=1}^{S} n_{ij}\sum_{i=1}^{S} n_{ik}}$$

where

$$\lambda_1 = \frac{\sum_{i=1}^{S}(n_{ij}(n_{ij}-1))}{\sum_{i=1}^{S} n_{ij}\left(\sum_{i=1}^{S} n_{ij} - 1\right)}$$

$$\lambda_2 = \frac{\sum_{i=1}^{S}(n_{ik}(n_{ik}-1))}{\sum_{i=1}^{S} n_{ik}\left(\sum_{i=1}^{S} n_{ij} - 1\right)}$$

where n_{ij} is the individuals of phylotype i in sample j, n_{ik} is the number of individuals of phylotype i in sample k (Morisita, 1959) and S is the total number of phylotypes. The Morisita indices of similarity were further analysed by cluster analysis using the PAST program (Hammer *et al.*, 2001).

Results

The clone names used indicate the sample site and library identification. The names begin with the letters KZNMV (for Kazan MV), followed by a number showing the layer used to construct the library (0, 5, 10, 25, 30 cm b.s.f.). A or B indicates *Archaea* and *Bacteria*, respectively. Surface sampling was actually conducted in the 0–1-cm layer and, for simplicity, it is coded as 0 in the phylotype names and annotated as the 'surface layer' in the text.

Archaea

A total of 242 archaeal 16S rRNA gene sequences were retrieved, and these were attributed to 38 phylotypes (see Supporting Information, Table S1). The vast majority (99.2%) of the archaeal sequences belonged to the *Euryarchaeota* (Fig. 1). Only one *Crenarchaeota* phylotype (KZNMV-10-A9, 4.1%) was found. This phylotype belonged to the marine benthic group B (MBG-B), whose members have been found in marine sediments and hydrothermal vent samples.

The surface layer was dominated by ANME-2 (KZNMV-0-A18, KZNMV-0-A25, KZNMV-0-A40, 89.1%). KZNMV-0-A18 was the most abundant phylotype in this layer and clustered within the ANME-2c subgroup. At 10 cm b.s.f., ANME-2 phylotypes again dominated (KZNMV-10-A2,

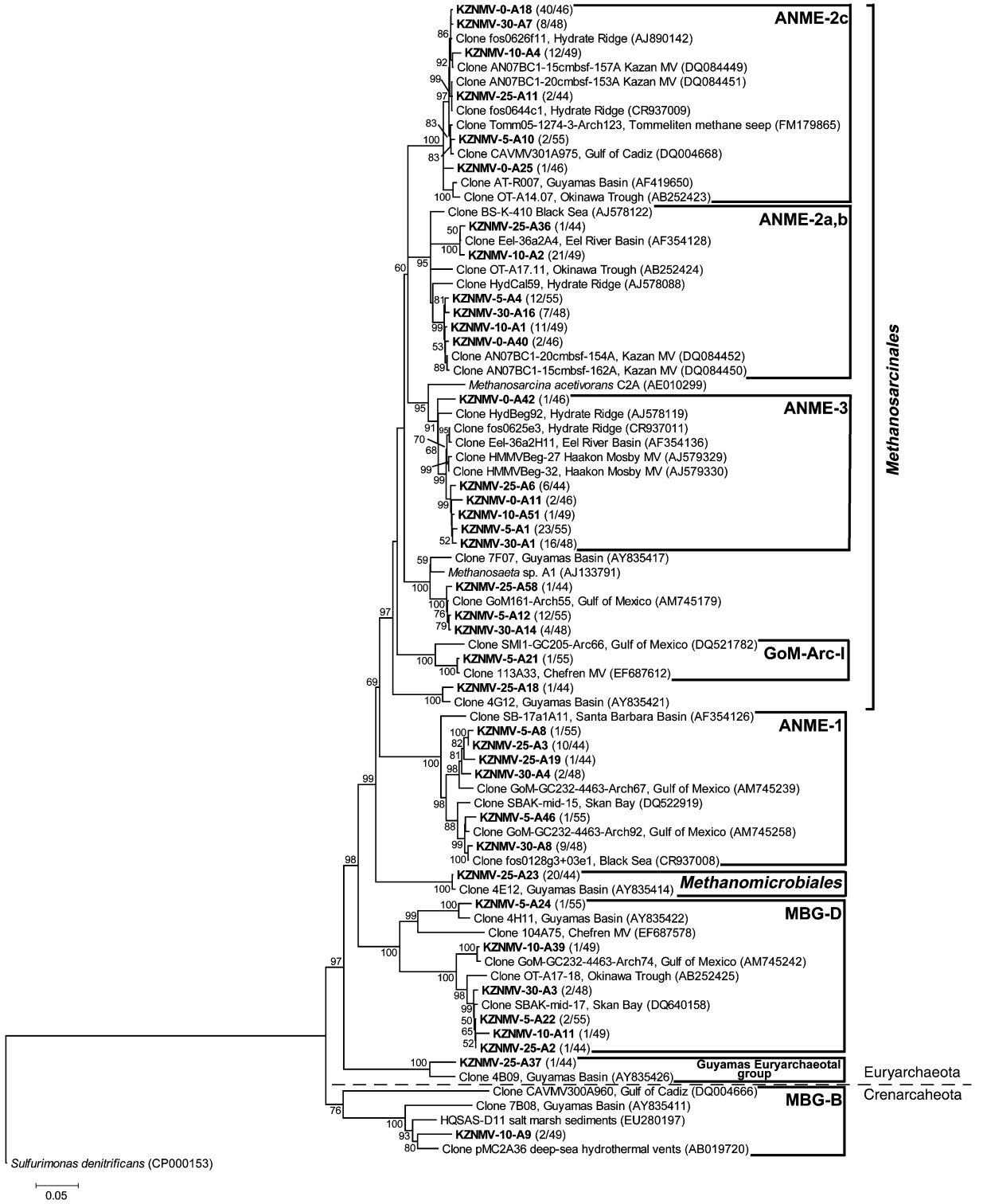

Fig. 1. Phylogenetic tree of the PCR-amplified archaeal 16S rRNA gene phylotypes (*c.* 1400 bp) in the sediments of the Kazan MV, East Mediterranean Sea, based on the neighbour-joining method as determined by distance using Kimura's two-parameter correction. Each phylotype recovered (in bold letters) is named after the sediment depth origin. Numbers of identical ($\geq$98% sequence similarity) phylotypes of the total number phylotypes found in this sediment depth are shown in parentheses. One thousand bootstrap analyses (distance) were conducted, and percentages $>$ 50% are indicated at nodes. Numbers in brackets are GenBank accession numbers. Scale bar represents 5% estimated distance.

KZNMV-10-A1, KZNMV-10-A4, 89.8%). Here, the most abundant phylotype, KZNMV-10-A2, was affiliated to the ANME-2a,b subgroup.

A group of five highly similar (> 98%) phylotypes (KZNMV-5-A1, KZNMV-30-A1, KZNMV-25-A6, KZNMV-0-A11, KZNMV-10-A1) belonged to the ANME-3 group. Phylotypes KZNMV-5-A1 and KZNMV-30-A1 dominated at 5 cm b.s.f. (41.8%) and 30 cm b.s.f. (33.3%), respectively. One single phylotype (KZNMV-0-A42) also belonged to the ANME-3 group.

At 25 cm b.s.f., the most abundant phylotype, KZNMV-25-A23 (45.5%), grouped within the *Methanomicrobiales* and was closely related (bootstrap value 100) to phylotype 4E12 from Guaymas Basin sediments. Members of the ANME-1 were also found. They occurred at 5 cm b.s.f (3.6%), 25 cm b.s.f (22.5%) and 30 cm b.s.f (25.0%).

Phylotypes KZNMV-5-A12 (21.8%), KZNMV-30-A14 (8.3%) and KZNMV-25-A58 (4.6%) converged (bootstrap value 100) with a monophyletic group of *Methanosaeta* spp. Six phylotypes with low abundance, from all except surface layers, belonged to the MBG-D and one from 5 cm b.s.f. was affiliated to GoM-Arc-I (Table 1, Fig. 1a). Finally, a singleton phylotype from 25 cm b.s.f. was related to the 'Guaymas Euryarchaeotal Group' (GEG).

Table 1. Phylogenetic grouping and relative abundance (%) of the phylotypes found at the Kazan MV, East Mediterranean Sea

	0 cm b.s.f. (68)	5 cm b.s.f. (89)	10 cm b.s.f. (87)	15 cm b.s.f.* (69)	20 cm b.s.f.* (79)	25 cm b.s.f. (55)	30 cm b.s.f. (75)
Bacteria							
Alphaproteobacteria	1.5	1.1	5.7	0.0	0.0	3.6	10.7
Betaproteobacteria	0.0	0.0	0.0	0.0	0.0	0.0	5.3
Gammaproteobacteria	51.5	1.1	25.3	0.0	0.0	32.7	40.0
Deltaproteobacteria	20.6	68.5	25.3	58.0	53.2	14.5	2.7
Epsilonproteobacteria	4.4	0.0	11.5	0.0	0.0	5.5	5.3
Acidobacteria	5.9	2.2	4.6	0.0	0.0	0.0	1.3
Actinobacteria	1.5	1.1	3.4	4.3	5.1	5.5	8.0
Bacteroidetes	2.9	1.1	1.1	0.0	0.0	1.8	0.0
Chlorobi	0.0	0.0	1.1	0.0	0.0	0.0	0.0
Chloroflexi	0.0	1.1	4.6	0.0	0.0	21.8	1.3
Deferribacteres	0.0	2.2	3.4	0.0	0.0	1.8	0.0
Firmicutes	1.5	0.0	1.1	0.0	0.0	0.0	12.0
Fusobacteria	0.0	0.0	0.0	0.0	0.0	0.0	1.3
JS1	1.5	7.9	2.3	0.0	0.0	1.8	2.7
OP11	0.0	1.1	3.4	7.2	7.6	0.0	0.0
OP8	0.0	2.2	3.4	0.0	0.0	0.0	0.0
Planctomycetes	1.5	2.2	1.1	0.0	0.0	3.6	0.0
Spirochaetes	0.0	0.0	0.0	7.2	2.5	0.0	0.0
TG1	0.0	0.0	0.0	0.0	0.0	1.8	0.0
WS2	0.0	1.1	0.0	0.0	0.0	0.0	0.0
WS3	4.4	2.2	1.1	23.2	31.6	0.0	0.0
Unaffiliated	2.9	4.9	1.1	0.0	0.0	5.5	9.3
	(46)	(55)	(49)	(43)	(49)	(44)	(48)
Archaea							
ANME-1	0.0	3.6	0.0	0.0	0.0	25.0	22.9
ANME-2a,b	4.3	21.8	65.3	16.3	36.7	2.3	14.6
ANME-2c	89.1	3.6	24.5	83.7	63.3	4.5	16.7
ANME-3	6.5	41.8	2.0	0.0	0.0	13.6	33.3
GEG	0.0	0.0	0.0	0.0	0.0	2.3	0.0
GoM Arc I	0.0	1.8	0.0	0.0	0.0	0.0	0.0
MBG-D	0.0	5.5	4.1	0.0	0.0	2.3	4.2
Methanomicrobiales	0.0	0.0	0.0	0.0	0.0	45.5	0.0
Methanosaeta-related	0.0	21.8	0.0	0.0	0.0	2.3	8.3
Methanosarcinales							
Unaffiliated *Methanosarcinales*	0.0	0.0	0.0	0.0	0.0	2.3	0.0
MBG-B	0.0	0.0	4.1	0.0	0.0	0.0	0.0

The total number of clones analysed in each library is given in parentheses.
*Kormas *et al*. (2008).

Bacteria

A total of 374 bacterial 16S rRNA gene sequences were retrieved, and these represented 205 unique phylotypes (Table S1). Phylotypes from the five subdivisions of the *Proteobacteria* accounted for the majority of sequences in each clone library, but not all subdivisions were retrieved in each layer (Figs 2 and 3). The remaining phylotypes were affiliated to 10 known phyla [*Acidobacteria*, *Actinobacteria*,

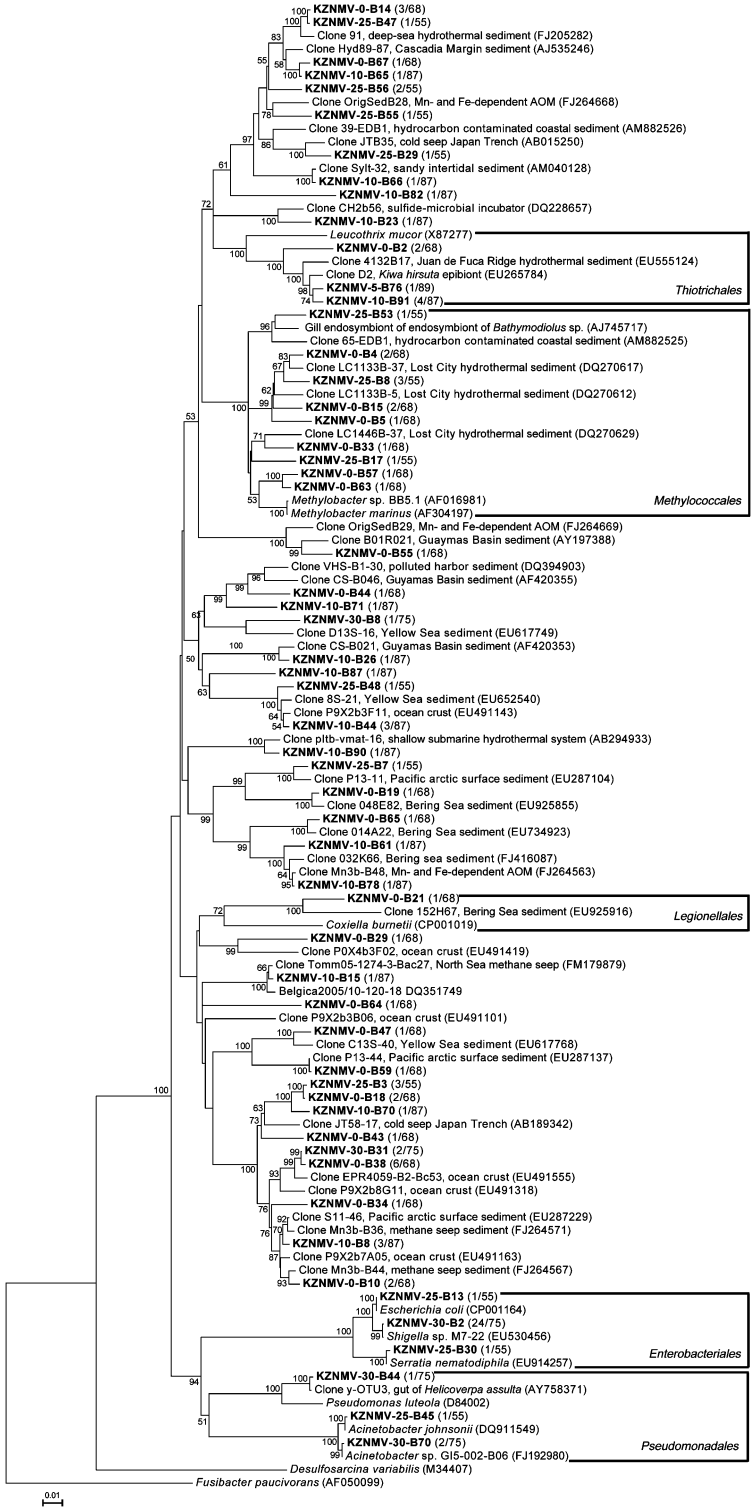

Fig. 2. Phylogenetic tree of the PCR-amplified *Gammaproteobacteria* – except from the outgroup sequence of the *Firmicutes Fusibacter paucivorans* – 16S rRNA gene phylotypes (*c.* 1400 bp) in the sediments of the Kazan MV, East Mediterranean Sea, based on the neighbour-joining method as determined by distance using Kimura's two-parameter correction. Each phylotype recovered (in bold letters) is named after the sediment depth origin. Numbers of identical (≥98% sequence similarity) phylotypes of the total number of phylotypes found in this sediment depth are shown in parentheses. One thousand bootstrap analyses (distance) were conducted, and percentages > 50% are indicated at nodes. Numbers in brackets are GenBank accession numbers. Scale bar represents 1% estimated distance.

Bacteroidetes, *Chlorobi*, *Chloroflexi*, *Deferribacteres*, *Firmicutes*, *Fusobacteria*, *Planctomycetes*, *Elusimicrobia* or Termite Group 1 (TG1)], five candidate divisions (JS1, OP8, OP11, WS2, WS3) and three unaffiliated groups (Fig. 4).

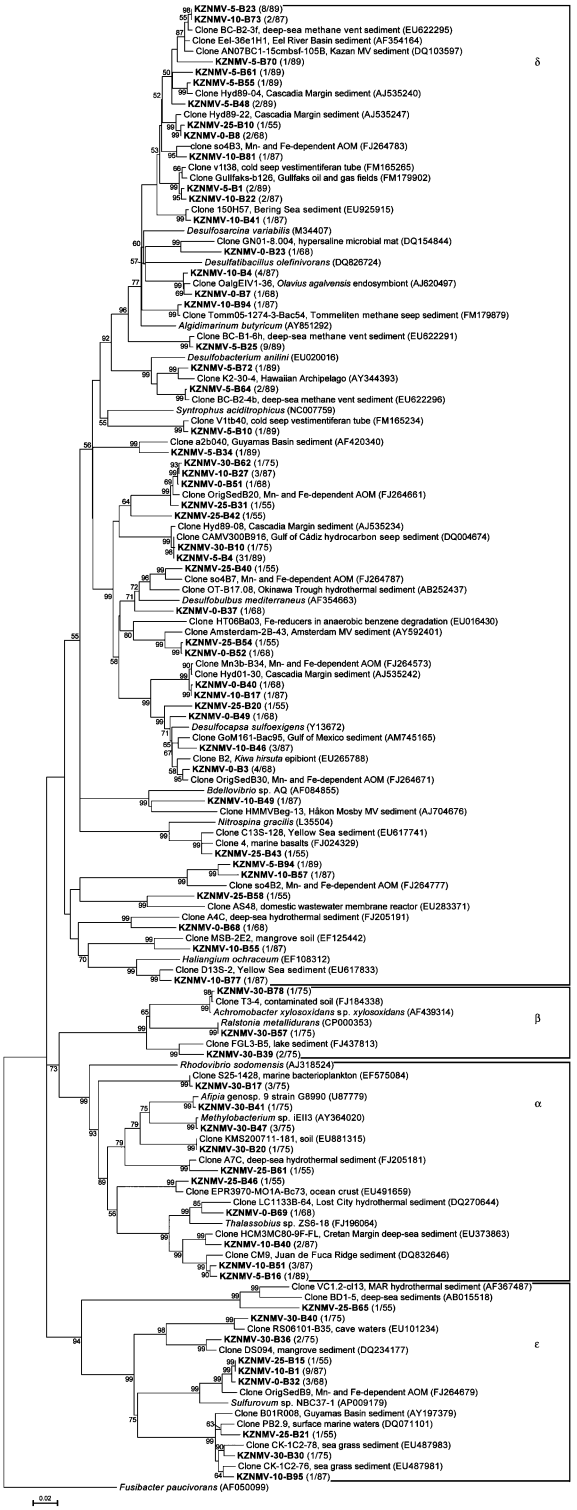

The *Gammaproteobacteria* phylotypes (Fig. 2) dominated (51.5%) the surface layer, and 30 cm b.s.f. (40.0%) and 25 cm b.s.f. (32.7%) layers. The *Gammaproteobacteria* codominated at 10 cm b.s.f. (25.3%), together with *Deltaproteobacteria*. The most abundant phylotype in each library was KZNMV-0-B38 (8.8%), KZNMV-30-B2 (32.0%) and KZNMV-10-B1 (10.3%), respectively.

Phylotypes of the *Deltaproteobacteria* (Fig. 3) dominated the 5 cm b.s.f. layer (68.5%). The dominant phylotype, KZNMV-5-B4 (34.8%), clustered within an as yet uncharacterized clade of *Desulfobulbaceae*. Phylotypes affiliated with the *Deltaproteobacteria* also occurred at 10 cm b.s.f. (25.3%), 0 cm b.s.f. (20.6%) and 25 cm b.s.f. (14.5%). Most of these phylotypes fell within SRB groups. At 30 cm b.s.f., only 2.7% of the phylotypes belonged to the *Deltaproteobacteria*.

Betaproteobacteria (Fig. 3) were only observed at 30 cm b.s.f. Three phylotypes, KZNMV-30-B38, KZNMV-30-B57 and KZNMV-30-B78, comprised 5.3% of the phylotypes at this layer.

The *Alphaproteobacteria* (Fig. 3) exhibited their highest abundance (10.7%) at 30 cm b.s.f. Moreover, three of four KZNMV-30 phylotypes affiliated with the *Alphaproteobacteria* formed a distinct clade from the other phylotypes originating from the other layers. This clade included *Methylobacterium* sp., a known methylotroph. At 10 cm b.s.f., the percentage of *Alphaproteobacteria* phylotypes was 5.7%, at 25 cm b.s.f. was 3.6% and in the surface layer and at 5 cm b.s.f. was *c.* 1%.

Phylotypes of the *Epsilonproteobacteria* (Fig. 3) occurred at all, except for the 5 cm b.s.f. layer. At the surface, 25 and 30 cm b.s.f. layers, only ~5% of *Epsilonproteobacteria* of each library were found, whereas phylotypes from 10 cm b.s.f. reached 11.5%. The most abundant phylotype of *Epsilonproteobacteria* in this layer was KZNMV-10-B1, which was also found at 0 cm b.s.f. (KZNMV-0-B32) and at 25 cm b.s.f. (KZNMV-25-B21) clustered within the *Sulfurovum* sp. clade.

Among nonproteobacterial phylotypes (Fig. 4), sequences belonging to candidate division JS1 were present in all bacterial 16S rRNA gene libraries constructed in this study.

Fig. 3. Phylogenetic tree of the PCR-amplified *Alpha-*, *Beta-*, *Delta-*, *Gamma-* and *Epsilonproteobacteria* 16S rRNA gene phylotypes (*c.* 1400 bp) in the sediments of the Kazan MV, East Mediterranean Sea, based on the neighbour-joining method as determined by distance using Kimura's two-parameter correction. Each phylotype recovered (in bold letters) is named after the sediment depth origin. Numbers of identical (≥98% sequence similarity) phylotypes of the total number of phylotypes found in this sediment depth are shown in parentheses. One thousand bootstrap analyses (distance) were conducted, and percentages > 50% are indicated at nodes. Numbers in brackets are GenBank accession numbers. Scale bar represents 2% estimated distance.

JS1 phylotypes from all examined depths represented a single phylotype and appeared to be elevated in the 5 cm b.s.f. layer (7.9%).

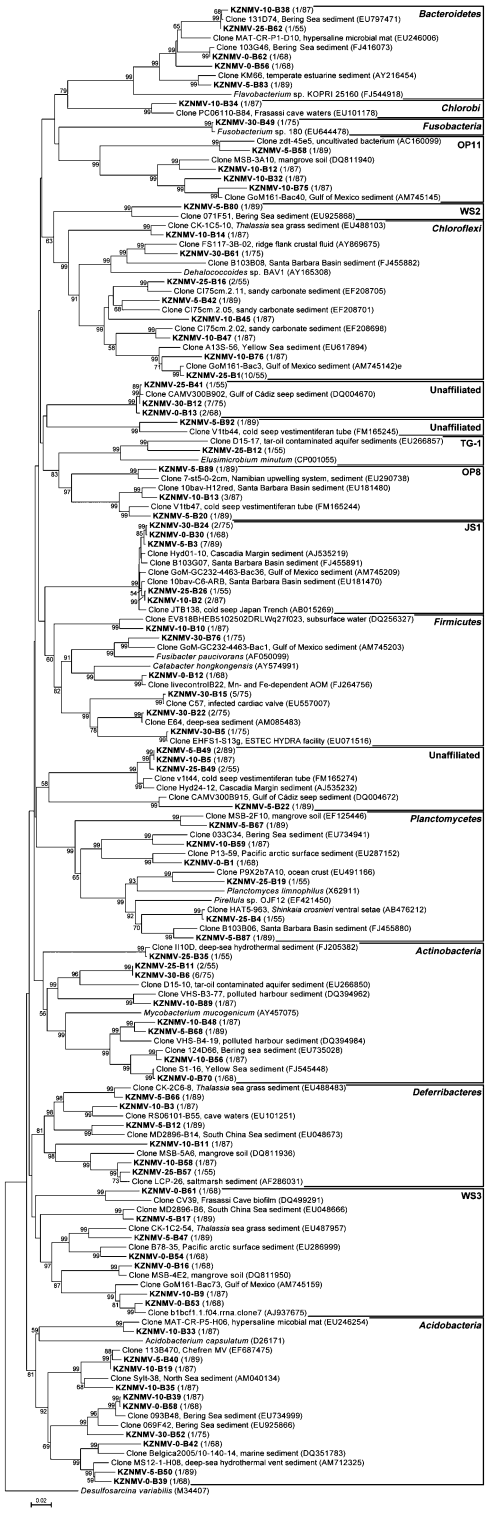

Members of the *Chloroflexi* were abundant in the 25 cm b.s.f. layer (21.8%). The dominant phylotype in this layer, KZNMV-25-1, was closely related (99% similarity) to sequences found in cold seep sediment from the Gulf of Mexico. Sequences of *Chloroflexi* were recovered from all examined depths, except the surface layer.

Sequences affiliated to the *Firmicutes* were found mostly in the 30 cm b.s.f. layer (12%), whereas they appeared in small numbers at the surface (1.5%) and 10 cm b.s.f. (1.1%) layers.

Similarity and diversity indices

The Morisita index of similarity was applied at the phylotype and phylogenetic group (i.e. phylum) level. The index for the bacterial communities was < 0.30, except for the 15 and 20 cm b.s.f. layers, at the phylotype level (Fig. 5a). This indicated little overlap among the bacterial phylotypes across these samples, and revealed that each sediment layer harboured a unique community of *Bacteria*. However, at the phylum level (Fig. 5b), the Morisita index was, on several occasions, higher (*c.* > 0.75). Clustering of the bacterial communities showed four distinct clusters: 1/30, 10/25, 15/20 and 5 cm b.s.f. (the last being close to the 15/20 cm b.s.f. cluster).

The Morisita clustering for *Archaea* exhibited a similar pattern (*c.* > 0.20) at both the phylotype and the phylum level (Figs 5c and d). The surface layer was closely related to the 15/20 cm b.s.f. layers and distantly related (*c.* 0.5) to the 10 cm b.s.f. layer. Another cluster was formed from the 5/30 cm b.s.f. layers, while the 25 cm b.s.f. layer did not cluster with any of the other layers.

The Shannon–Wiener diversity index *H* at all examined depths was higher for *Bacteria* (1.47–3.82) than for *Archaea* (0.56–1.73) (Fig. 6). Changes in *H* with depth were not consistent between archaeal and bacterial clone libraries. The 15 and 20 cm b.s.f. layers appeared to represent a local minimum for both archaeal and bacterial diversity indices. *Archaea* exhibited the lowest *H*-value at the 15 cm b.s.f. layer, followed by the surface and 20 cm b.s.f. layers. At all the remaining layers, *H* was two to three times higher. *Bacteria*,

Fig. 4. Phylogenetic tree of PCR-amplified of bacterial (except all *Proteobacteria*) 16S rRNA gene phylotypes (*c.* 1400 bp) in the sediments of the Kazan MV, East Mediterranean Sea, based on the neighbour-joining method as determined by distance using Kimura's two-parameter correction. Each phylotype recovered (in bold letters) is named after the sediment depth origin. Numbers of identical ($\geq$98% sequence similarity) phylotypes of the total number phylotypes found in this sediment depth are shown in parentheses. One thousand bootstrap analyses (distance) were conducted, and percentages $> 50\%$ are indicated at nodes. Numbers in brackets are GenBank accession numbers. Scale bar represents 2% estimated distance.

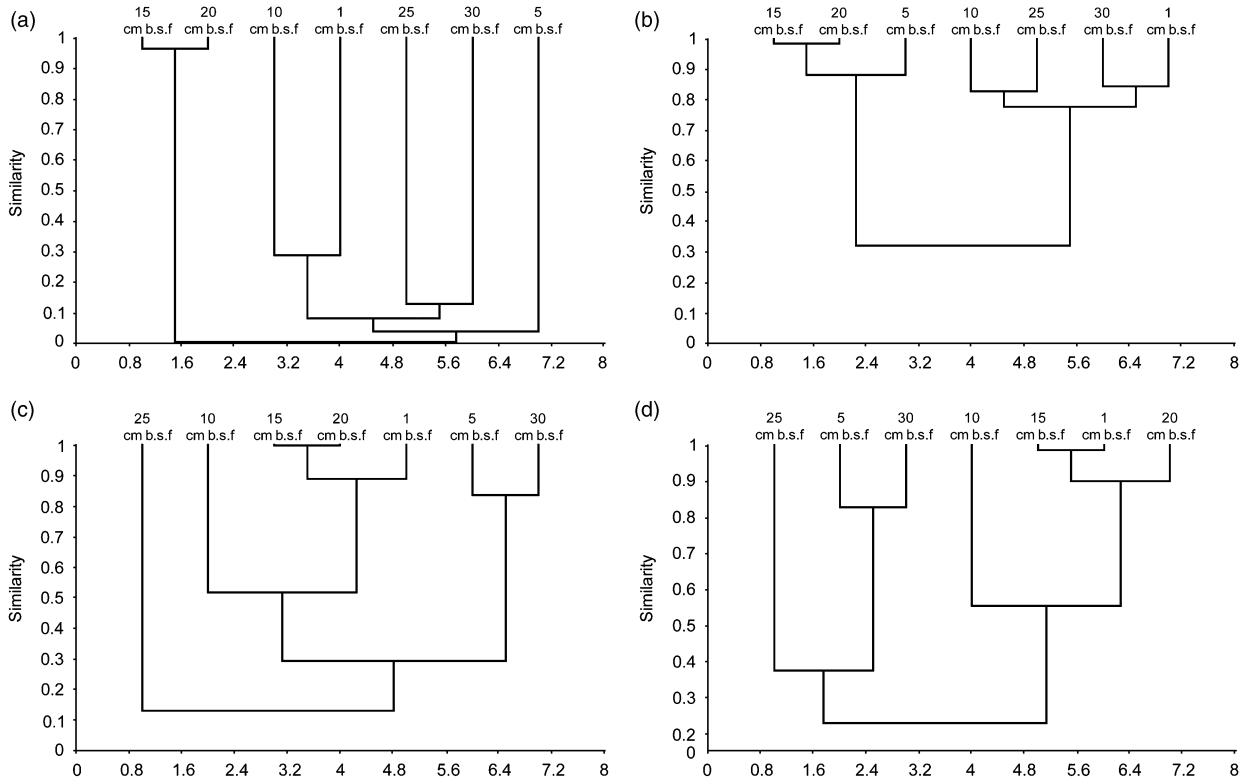

Fig. 5. Cluster analysis based on the Morisita similarity index for the (a) bacterial and (c) archaeal 16S rRNA gene phylotypes, and (b) bacterial and archaeal (d) groups, from sediments of the Kazan MV, East Mediterranean Sea.

on the other hand, showed the maximum *H* diversity at 10 cm b.s.f., but this was roughly comparable with the 1 and 25 cm b.s.f. layers. The Pielou evenness index *J* (Fig. 6) varied between 0.35 and 0.95 (average 0.71) for *Archaea* and between 0.76 and 0.96 (average 0.87) for *Bacteria*, and was higher for *Archaea* only in the 20 and 30 cm b.s.f. layers. These values of *J* indicate that the bacterial clone libraries showed a more even distribution of phylotypes than the archaeal libraries.

Discussion

We investigated the diversity of *Bacteria* and *Archaea* at a high sediment depth resolution in the Kazan MV, East Mediterranean Sea. Although we took all the necessary steps to minimize the nonquantitative effects of PCR (Bohannan & Hughes, 2003), the innate limitations of the PCR-based approach remain and thus our data refer to the apparent richness of phylotypes and the microorganisms that they represent. Coverage of the clone libraries according to Good's *C* estimator (Kemp & Aller, 2004) was more satisfactory for the *Archaea* (>0.8) than for the *Bacteria* (*c.* 0.4–0.8) (Fig. 7). This implies that the majority of the *Archaea* phylotypes have been identified, but for the *Bacteria*, only the most abundant and several of the low-abundance (i.e. singletons and doubletons) phylotypes have been retrieved. This is also reflected in the higher number of bacterial singletons than archaeal singletons (Table S1). Revealing such rare phylotypes in complex communities is important. Rare species are thought to grow slow (they would otherwise become common), but in habitats such as MVs and deep-sea sediments, all microbial growth is slow (Fuhrman, 2009). For example, although ANMEs metabolize methane quite quickly (Nauhaus *et al.*, 2005) their growth is slow. Thus, the functional role of rare species in the Kazan MV might be more important than it is in other, more productive habitats such as the upper marine water column. Moreover, the coexistence of rare with abundant phylotypes can serve as a 'seed-bank' for future perturbations (Pedrós-Alió, 2006), for example after mud fluid eruptions.

Community composition

The relative dominance of *Euryarchaeota* over *Crenarchaeota* in all layers has been reported for other gas-hydrate- or methane-bearing sediments as well (e.g. Inagaki *et al.*, 2006; Parkes *et al.*, 2007). The *Euryarchaeota* found were related to

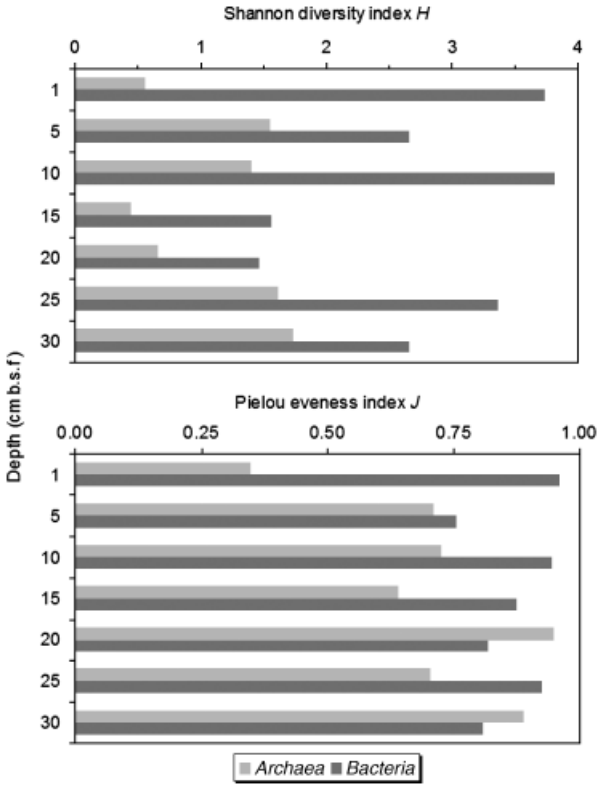

Fig. 6. Shannon diversity index *H* and Pielou evenness index *J* for the bacterial and archaeal 16S rRNA gene clone libraries from sediments of the Kazan MV, East Mediterranean Sea.

methane metabolism. In particular, ANME groups were retrieved at a high relative abundance (> 50%) in all depth layers. At 25 cm b.s.f., the dominant phylotype (KZNMV-25-A23) was closely related to the H_2-using methanogen *Methanogenium marinum*. Therefore, the archaeal communities of the top 30 cm in the Kazan MV are highly specialized and selected for life within gas-hydrate sediments. The fact that high concentrations of gas hydrate of the size of rice grains were present even close to the sediment surface can be interpreted as a very strong methane flux (Perissoratis, 2005), providing suitable substrate conditions for ANME.

The *Deltaproteobacteria* found were highly diverse (Fig. 3), even at the order level (*Desulfobacterales*, *Synthrophobacterales*, *Bdellovibrionales* and *Myxococcales*). Many phylotypes found at 5 cm b.s.f. fell into the cold seep-associated clades of SRB, SEEP-SRB1 (*Desulfosarcina*/*Desulfococcus*-related), SEEP-SRB3 (*Desulfobulbus*-related) and SEEP-SRB4 (*Desulforhopalus*-related). Members of SEEP-SRB1 are considered to be the sulphate-reducing partners of ANME-1 and ANME-2 (Knittel *et al.*, 2003), while the ecological role of SEEP-SRB3 and SEEP-SRB4 remains unknown. The most abundant phylotype (KZNMV-5-B4, 50.8% of the *Deltaproteobacteria* phylotypes) was clustered within an as yet uncharacterized clade of *Desulfobulbaceae*, which is physically associated with ANME-2c consortia (Pernthaler *et al.*, 2008). In addition, a few phylotypes were related to *Desulfobacterium anilii* and related environmental sequences. This group is known to include several cultivated and uncultivated hydrocarbon-degrading *Bacteria* capable of complete oxidation of various aromatic hydrocarbons (Harms *et al.*, 1999).

Non-SRB sequences of the *Deltaproteobacteria* were also present at all depths. Phylotype KZNMV-10-B49 was related to *Bdellovibrio* sp. and *Bacteriovorax* sp. Both genera are aerobic, obligatory predators of *Bacteria* that forage on a wide variety of susceptible gram-negative microorganisms (Baer *et al.*, 2000). Four phylotypes fell into the *Myxococcales*, a group often found in marine sediments (Ravenschlag *et al.*, 1999; Wilms *et al.*, 2006; Zhang *et al.*, 2008). Members of this group are known nonobligate predators as well (Burnham *et al.*, 1984). Finally, a singleton phylotype (KZNMV-5-B10) was related to *Syntrophus aciditrophus*, known to ferment benzoate and living often syntrophically with H_2-consuming methanogens (Jackson *et al.*, 1999; Becker *et al.*, 2005).

Based on the archaeal and *Deltaproteobacteria* phylotypes found, the prokaryotic communities of the Kazan MV sediments consist of microorganisms involved in methane- and, presumably, sulphate-based biogeochemical processes, as is the case for the eastern Mediterranean MV cold seep sediments (Heijs *et al.*, 2006, 2007; Kormas *et al.*, 2008; Omoregie *et al.*, 2008, 2009). The geochemical profiles (Kormas *et al.*, 2008) support the notion that AOM is a metabolic process than takes place at 15 and 20 cm b.s.f., whereas earlier studies placed the AOM zone at the 7–20 cm b.s.f. (Werne *et al.*, 2002, 2004; Haese *et al.*, 2003).

The sequences of *Gammaproteobacteria* represented diverse organisms (Fig. 2), as is the case in several marine sediments (Li *et al.*, 1999; Inagaki *et al.*, 2003; Bowman *et al.*, 2005). The dominance of this group has been observed in another case of gas-hydrate sediment and was attributed to the opportunistic life strategies of the *Gammaproteobacteria* (Jiang *et al.*, 2007). Their ecophysiological role is also diverse, but several of the phylotypes recovered by this study were related to characterized sulphur and sulphide oxidizers or to environmental sequences originating from habitats where sulphur and sulphide oxidation occurred or was predicted to occur.

Phylotypes most closely aligned with psychrophilic *Legionellales* primarily isolated from deep-sea environments were also recovered. Other phylotypes belonging to families that are more physiologically constrained include the methane-oxidizing *Methylococcaceae* (*Methylococcales*) (e.g. KZNMV-0-B63, KZNMV-0-B33), which were found mainly at the top layer, as well as at 10 and 25 cm b.s.f., while

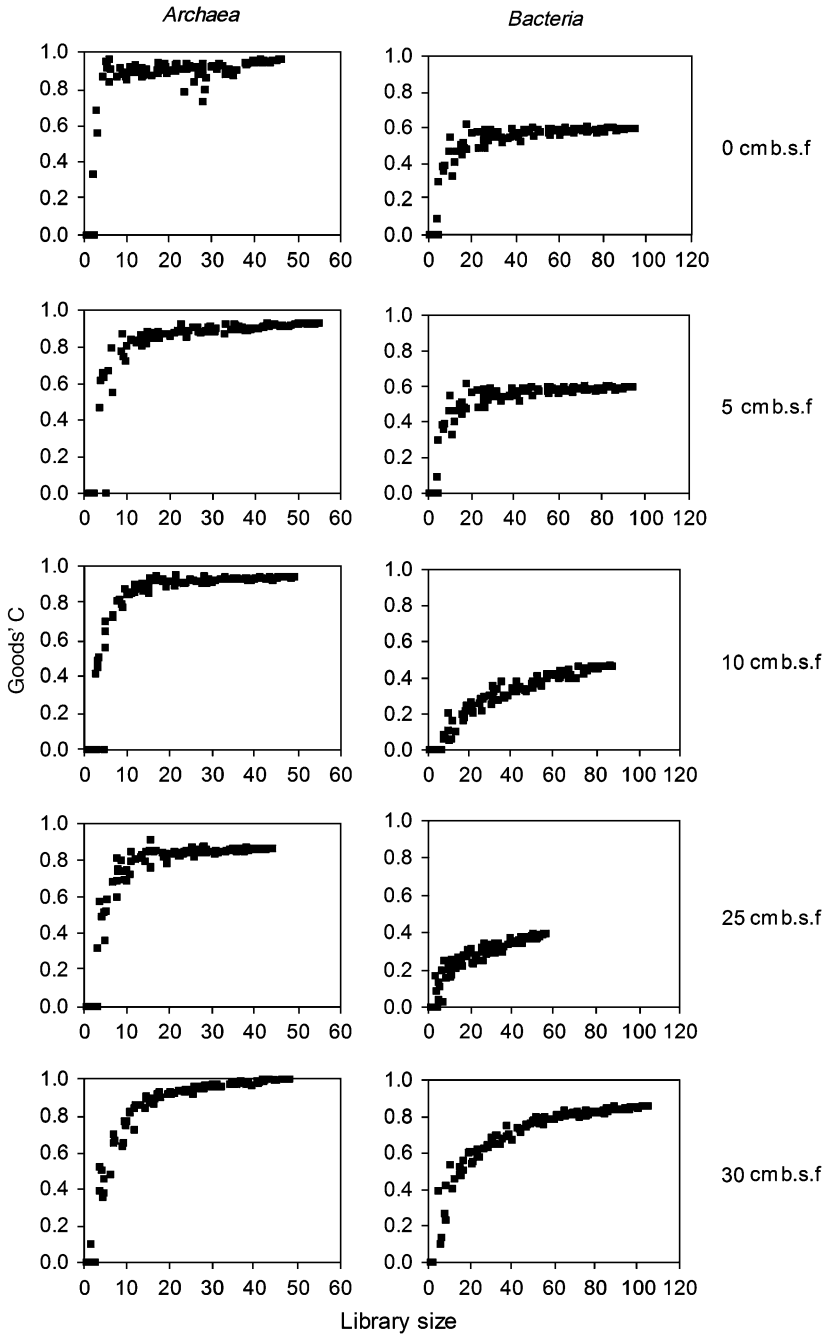

Fig. 7. Clone library coverage based on Good's *C* estimator of the prokaryotic 16S rRNA gene libraries from the Kazan MV, East Mediterranean Sea.

sulphide-oxidizing *Ectothiorhodospiraceae* (*Chromatiales*) (KZNMV-0-B47 and KZNMV-0-B59) were only retrieved from the top layer. The rest of the phylotypes from the top, 10 and 25 cm b.s.f. layers belonged to the orders of *Pseudomonadales*, *Enterobacterales*, *Legionellales* and *Thiotrichales* or formed clusters that could not be firmly affiliated to any known taxonomic groups within the *Gammaproteobacteria* and included only uncultured representatives. These uncharacterized groups, however, were clustered with phylotypes recovered from cold seep environments, gas-hydrate-associated sediments, ocean crusts, marine sediments, characterized symbionts–epibionts of marine invertebrates and putative sulphur oxidizers, implying their involvement in the sulphur cycle.

The *Epsilonproteobacteria* phylotypes found in this work were related to phylotypes from deep-sea sediments, hydrothermal vents, cave waters and cold seeps. The only cultured isolate within this clade is *Sulfurovum lithotrophicum*, a

sulphur-oxidizing chemolithoautotroph from hydrothermal sediments in a black smoker environment (Inagaki *et al.*, 2004). Thus, *Epsilonproteobacteria* in the Kazan MV sediment were probably involved, together with *Gammaproteobacteria*, in sulphur cycling. Indeed, the composition of major elements in the sediments of the Anaximander MVs showed a clear enrichment in sulphur compared with the general composition of pelagic sediments of the East Mediterranean Sea (Perissoratis, 2005).

The site studied was characterized by the absence of overlying pelagic sediments, indicative of relatively recent mud flows, suggesting possible oxygen diffusion down to the sediment. At the bottom of the core (35–40 cm b.s.f.), larger hydrates were found. The possible outcropping of these hydrates could cause sediment resuspension and mixing, thus enhancing oxygen diffusion from the sediment surface and creation of microaerophilic conditions. This would also explain the presence and possible metabolic activity of aerobic, methylotrophic *Alphaproteobacteria* at the bottom (30 cm b.s.f.) layer. Moreover, methylotrophs form different kinds of resting stages such as cysts and endospores, which enables them to survive even long periods of anoxia or lack of methane (Whittenbury *et al.*, 1970).

Among the nonproteobacterial phylotypes, sequences belonging to phylogenetic groups related to deep biosphere and gas hydrate sediments were retrieved. The same JS1 phylotype was present in all layers. Originally identified in Japan Sea sediments, members of candidate division JS1 have also been commonly recovered from methane-hydrate-associated marine sediments, such as sediments from the Nankai Trough, Hydrate Ridge and the Peru Margin (Webster *et al.*, 2004, 2006, 2007; Fry *et al.*, 2006; Inagaki *et al.*, 2006; Parkes *et al.*, 2007), but also from older Kazan MV sediments (Heijs *et al.*, 2008). Sequences of *Chloroflexi* were recovered from all examined depths, except the top one, and were present in greatest abundance in our clone library from the 25 cm b.s.f. layer. *Chloroflexi* occur frequently in hydrocarbon-rich sediments and the deep subsurface (Kormas *et al.*, 2003; Inagaki *et al.*, 2006).

Diversity patterns

Cluster analysis was performed to reveal community similarity patterns, at both the phylotype and the phylogenetic group levels, between the different sediment layers. The results from both phylotype and phylum approaches were in agreement for the *Archaea* (Fig. 5c and d). For the *Bacteria* (Fig. 5a and b), however, the different layers showed different community similarities under the two different approaches. When phylotypes, especially the most abundant and/or the most dominant ones, are affiliated to a large, functionally diverse group (e.g. *Gammaproteobacteria*), cluster analysis may lead to 'false' community similarities (e.g. between the surface and the 30 cm b.s.f. layers). This highlights the need for diversity comparisons at the phylotype rather than at the phylum level, and that higher taxon analysis is appropriate only in highly specific communities.

The use of the Shannon–Wiener diversity index H in prokaryotic communities seems to be applicable and realistically informative, when clone library coverage is sufficiently large (Hill *et al.*, 2003; Kemp & Aller, 2004), and can be used to compare the diversity between different sites or even studies. In addition, the application of such a universal index, which is fairly easily applied in meta-analysis of published data, will allow reasonable comparisons between hot-spot and non-hot-spot sites. In our study, the minimal H-values for both the *Bacteria* and the *Archaea* at 15/20 cm b.s.f. was further evidence that a unique, specialized assemblage was established there, related to AOM according to the inferred ecophysiology of the phylotypes found. Another pattern revealed was that the H-values for *Bacteria* and *Archaea* were lower than for previous works from sediments of the same and other MVs (Amsterdam and Napoli) in the eastern Mediterranean (Heijs *et al.*, 2008), even though in that study, the more coarse vertical selection of the extracted sediment may have affected the overall values, but were comparable with hydrate sediments from the Gulf of Mexico (Mills *et al.*, 2005). Bacterial diversity was greater than archaeal diversity for all layers, which is generally the case for bacterial and archaeal libraries constructed from the same sampling location (Aller & Kemp, 2008). The higher bacterial vs. archaeal diversity seems to apply to hydrate-bearing sediments (Mills *et al.*, 2005), cold seeps (Reed *et al.*, 2006) and MVs (Heijs *et al.*, 2008), and is possibly a general trend in methane-related environments (Lanoil *et al.*, 2001; Aloisi *et al.*, 2002; Teske *et al.*, 2002; Nauhaus *et al.*, 2005; Lloyd *et al.*, 2006; Lösekann *et al.*, 2007) based on the relative abundance of phylotypes retrieved from each domain. The different ecophysiological roles of *Bacteria* and *Archaea* might primarily involve the use of available energy sources and adaptation to energy stress (Valentine, 2007). For methane oxidizers, extensive environmental, laboratory and modelling studies indicate that their mode of growth yields only small amounts of energy and often occurs at exceedingly slow rates. Valentine (2007) contends that the distribution of catabolic pathways among the *Archaea* results directly from their adaptation to chronic energy stress and that distinctive mechanisms of energy conservation allow many *Archaea* to adapt readily to environments of differing energy availabilities. In the case of methanogens and methane oxidizers, dominance is achieved through metabolic exclusivity, whereby these organisms have evolved to exclude or outcompete bacteria by the use of unique catabolic pathways. *Bacteria*, by contrast, seem to focus on exploiting new or variable resources.

Deep-sea sediment geochemical and physical data are acquired at a fine spatial scale more often than biological samples. For marine MVs, the studies available are characterized by a general lack of data on the temporal changes of their hosted microbial communities. In the case of the Kazan MV, however, Heijs *et al.* (2008) analysed the prokaryotic diversity in samples taken in 1999 from a site *c.* 30 m away – but still in the active site of the MV – from the one we analysed. Heijs *et al.* (2008) used a coarser sampling depth resolution (0–6, 6–22 and 22–34 cm b.s.f.). In addition, the different sediment mass used for DNA extraction and different PCR conditions and primers limit the safety of such comparisons. Because of the scarcity of such data, however, we believe that a comparison of relative abundances is feasible, and after pooling our results according to the depth layers of 0–5, 10–20 and 25–30 cm b.s.f., the two studies revealed very different biodiversities, especially in the top two layers. For *Archaea*, the top layer was dominated by *Halobacteriales*-related phylotypes (Heijs *et al.*, 2008), but our study showed that it was dominated by ANME-2. The middle layer showed an overlap in ANME-2 (the second most dominant group in Heijs *et al.*, 2008), although with different phylotypes. The bottom layer was dominated by ANME-2 (Heijs *et al.*, 2008) and by ANME-1 and ANME-3 (present study). The dominant *Bacteria* in the top two layers were different in the two studies (*Actinobacteria*, *Chloroflexi* vs. *Gamma-* and *Deltaproteobacteria*). The bottom layer, although containing different dominant phyla in the two studies, showed some overlap for the *Deltaproteobacteria* and *Chloroflexi*. Such variations, apart from methodological and microscale differences, could be attributed to differences in the prevailing conditions, for example due to eruptions. We suggest that our sampling strategy revealed a higher prokaryotic diversity and also showed that the distribution of prokaryotes explains the geochemical features found. Future comparisons will confirm the persistent or the ephemeral aspect of these communities.

In conclusion, the present study showed that *Bacteria* and *Archaea* communities differ even every 5 cm of the top 30 cm in an active site of the Kazan MV with recent mud flow. The archaeal communities showed a lower diversity than the bacterial communities, but were more closely related to ANMEs, while the *Bacteria* included AOM-related phylotypes. Only at 15 and 20 cm b.s.f. did the two communities show the typical AOM-related profile, known to occur in similar habitats elsewhere, consistent with the prevailing methane–sulphate conditions.

Acknowledgements

This research project is cofinanced by the EU-European Social Fund (75%) and the Greek Ministry of Development – GSRT (25%). Sampling was conducted during the European Commission project ANAXIMANDER (contract no. EVK3-CT-2002-00068). The officers and crew of the R/V *AEGAEO* are gratefully acknowledged for their contribution to fieldwork and sampling. We thank two anonymous reviewers and Virginia P. Edgcomb for their critical reading of the manuscript.

References

Aller JY & Kemp PF (2008) Are Archaea inherently less diverse than Bacteria in the same environments? *FEMS Microbiol Ecol* **65**: 74–87.

Aloisi G, Pierre C, Rouchy JM, Foucher JP & Woodside J (2000) Methane-related authigenic carbonates of Eastern Mediterranean Sea mud volcanoes and their possible relation to gas hydrate destabilisation. *Earth Planet Sc Lett* **184**: 321–338.

Aloisi G, Bouloubassi I, Heijs SK, Pancost RD, Pierre C, Sinninghe Damsté JS, Gottschal JC, Forney LJ & Rouchy JM (2002) CH_4-consuming microorganisms and the formation of carbonate crusts at cold seeps. *Earth Planet Sc Lett* **203**: 195–203.

Ashelford KE, Chuzhanova NA, Fry JC, Jones AJ & Weightman AJ (2005) At least 1 in 20 16S rRNA sequence records currently held in public repositories is estimated to contain substantial anomalies. *Appl Environ Microb* **71**: 7724–7736.

Baer ML, Ravel J, Chun J, Hill RT & Williams HN (2000) A proposal for the reclassification of *Bdellovibrio stolpii* and *Bdellovibrio starrii* into a new genus, *Bacteriovorax* gen. nov. as *Bacteriovorax stolpii* comb. nov. and *Bacteriovorax starrii* comb. nov., respectively. *Int J Syst Evol Micr* **50**: 219–224.

Becker JG, Berardesco G, Rittmann BE & Stahl DA (2005) The role of syntrophic associations in sustaining anaerobic mineralization of chlorinated organic compounds. *Environ Health Persp* **113**: 310–316.

Boetius A & Suess E (2004) Hydrate ridge: a natural laboratory for the study of microbial life fueled by methane from near-surface gas hydrates. *Chem Geol* **205**: 291–310.

Bohannan BJM & Hughes J (2003) New approaches to analyzing microbial biodiversity data. *Curr Opin Microbiol* **6**: 282–287.

Bouloubassi I, Aloisi G, Pancost RD, Hopmans E, Pierre C & Sinninghe Damsté JS (2006) Archaeal and bacterial lipids in authigenic carbonate crusts from eastern Mediterranean mud volcanoes. *Org Geochem* **37**: 484–500.

Bowman JP, McCammon SA & Dann AL (2005) Biogeographic and quantitative analyses of abundant uncultivated γ-proteobacterial clades from marine sediment. *Microb Ecol* **49**: 451–460.

Burnham JC, Collart SA & Daft MJ (1984) Myxococcal predation of the cyanobacterium *Phormidium luridum* in aqueous environments. *Arch Microbiol* **137**: 220–225.

Charlou JL, Donval JP, Zitter T, Roy N, Jean-Baptiste P, Foucher JP & Woodside J (2003) Evidence of methane venting and

geochemistry of brines on mud volcanoes of the eastern Mediterranean Sea. *Deep-Sea Res Pt I* **50**: 941–958.

Cita MB, Ryan WBF & Paggi L (1981) Prometheus mud-breccia: an example of shale diapirism in the Western Mediterranean Ridge. *Ann Geol Pays Hellen* **30**: 543–570.

Cole JR, Chai B, Marsh TL *et al.* (2003) The Ribosomal Database Project (RDP-II): previewing a new autoaligner that allows regular updates and the new prokaryotic taxonomy. *Nucleic Acids Res* **31**: 442–443.

DeSantis TZ, Hugenholtz P, Keller K, Brodie EL, Larsen N, Piceno YM, Phan R & Andersen GL (2006) NAST: a multiple sequence alignment server for comparative analysis of 16S rRNA genes. *Nucleic Acids Res* **34**: 394–399.

Fields MW, Schryver JC, Brandt CC, Yan T, Zhou JZ & Palumbo AV (2006) Confidence intervals of similarity values determined for cloned SSU rRNA genes from environmental samples. *J Microbiol Meth* **65**: 144–152.

Fry JC, Webster G, Cragg BA, Weightman AJ & Parkes RJ (2006) Analysis of DGGE profiles to explore the relationship between prokaryotic community composition and biogeochemical processes in deep subseafloor sediments from the Peru Margin. *FEMS Microbiol Ecol* **58**: 86–98.

Fuhrman JA (2009) Microbial community structure and its functional implications. *Nature* **459**: 193–199.

Good IJ (1953) The population frequencies of species and the estimation of population parameters. *Biometrika* **40**: 237–264.

Haese RR, Meile C, Van Cappellen P & De Lange GJ (2003) Carbon geochemistry of cold seeps: methane fluxes and transformation in sediments from Kazan mud volcano, eastern Mediterranean Sea. *Earth Planet Sc Lett* **212**: 361–375.

Hallam SJ, Putnam N, Preston CM, Detter JC, Rokhsar D, Richardson PH & DeLong EF (2004) Reverse methanogenesis: testing the hypothesis with environmental genomics. *Science* **305**: 1457–1462.

Hammer Ø, Harper DAT & Ryan PD (2001) Past: paleontological statistics software package for education and data analysis. *Palaeontol Electron* **4**: 1–9.

Harms G, Zengler K, Rabus R, Aeckersberg F, Minz D, Rosselló-Mora R & Widdel F (1999) Anaerobic oxidation of *o*-xylene, *m*-xylene, and homologous alkylbenzenes by new types of sulfate-reducing bacteria. *Appl Environ Microb* **65**: 999–1004.

Heijs SK, Aloisi G, Bouloubassi I, Pancost RD, Pierre C, Sinninghe Damsté JS, Gottschal JC, Van Elsas JD & Forney LJ (2006) Microbial community structure in three deep-sea carbonate crusts. *Microb Ecol* **52**: 451–462.

Heijs SK, Haese RR, Van Der Wielen PWJJ, Forney LJ & Van Elsas JD (2007) Use of 16S rRNA gene based clone libraries to assess microbial communities potentially involved in anaerobic methane oxidation in a Mediterranean cold seep. *Microb Ecol* **53**: 384–398.

Heijs SK, Laverman AM, Forney LJ, Hardoim PR & Van Elsas JD (2008) Comparison of deep-sea sediment microbial communities in the Eastern Mediterranean. *FEMS Microbiol Ecol* **64**: 362–377.

Hill TCJ, Walsh KA, Harris JA & Moffett BF (2003) Using ecological diversity measures with bacterial communities. *FEMS Microbiol Ecol* **43**: 1–11.

Inagaki F, Suzuki M, Takai K, Oida H, Sakamoto T, Aoki K, Nealson KH & Horikoshi K (2003) Microbial communities associated with geological horizons in coastal subseafloor sediments from the Sea of Okhotsk. *Appl Environ Microb* **69**: 7224–7235.

Inagaki F, Takai K, Nealson KH & Horikoshi K (2004) *Sulfurovum lithotrophicum* gen. nov., sp. nov., a novel sulfur-oxidizing chemolithoautotroph within the ε-proteobacteria isolated from Okinawa Trough hydrothermal sediments. *Int J Syst Evol Micr* **54**: 1477–1482.

Inagaki F, Nunoura T, Nakagawa S *et al.* (2006) Biogeographical distribution and diversity of microbes in methane hydrate-bearing deep marine sediments on the Pacific Ocean Margin. *P Natl Acad Sci USA* **103**: 2815–2820.

Jackson BE, Bhupathiraju VK, Tanner RS, Woese CR & McInerney MJ (1999) *Syntrophus aciditrophicus* sp. nov., a new anaerobic bacterium that degrades fatty acids and benzoate in syntrophic association with hydrogen using microorganisms. *Arch Microbiol* **171**: 107–114.

Jiang H, Dong H, Ji S, Ye Y & Wu N (2007) Microbial diversity in the deep marine sediments from the Qiongdongnan Basin in South China Sea. *Geomicrobiol J* **24**: 505–517.

Kemp PF & Aller JY (2004) Estimating prokaryotic diversity: when are 16S rDNA libraries large enough? *Limnol Oceanogr-Meth* **2**: 114–125.

Knittel K, Boetius A, Lemke A, Eilers H, Lochte K, Pfannkuche O, Linke P & Amann R (2003) Activity, distribution, and diversity of sulfate reducers and other bacteria in sediments above gas hydrate (Cascadia Margin, Oregon). *Geomicrobiol J* **20**: 269–294.

Kormas KA, Smith DC, Edgcomb V & Teske A (2003) Molecular analysis of deep subsurface microbial communities in Nankai Trough sediments (ODP Leg 190, Site 1176). *FEMS Microbiol Ecol* **45**: 115–125.

Kormas KA, Meziti A, Dählmann A, De Lange GJ & Lykousis V (2008) Characterization of methanogenic and prokaryotic assemblages based on mcrA and 16S rRNA gene diversity in sediments of the Kazan mud volcano (Mediterranean Sea). *Geobiology* **6**: 450–460.

Lanoil BD, Sassen R, La Duc MT, Sweet ST & Nealson KH (2001) Bacteria and Archaea physically associated with Gulf of Mexico gas hydrates. *Appl Environ Microb* **67**: 5143–5153.

Li L, Kato C & Horikoshi K (1999) Bacterial diversity in deep-sea sediments from different depths. *Biodivers Conserv* **8**: 659–677.

Lloyd KG, Lapham L & Teske A (2006) An anaerobic methane-oxidizing community of ANME-1b archaea in hypersaline gulf of Mexico sediments. *Appl Environ Microb* **72**: 7218–7230.

Lösekann T, Knittel K, Nadalig T, Fuchs B, Niemann H, Boetius A & Amann R (2007) Diversity and abundance of aerobic and anaerobic methane oxidizers at the Haakon Mosby Mud Volcano, Barents Sea. *Appl Environ Microb* **73**: 3348–3362.

Lykousis V, Alexandri S, Woodside J *et al.* (2004) New evidence of extensive active mud volcanism in the Anaximander mountains (Eastern Mediterranean): the 'ATHINA' mud volcano. *Environ Geol* **46**: 1030–1037.

Lykousis V, Alexandri S, Woodside J *et al.* (2009) Mud volcanoes and gas hydrates in the Anaximander mountains (Eastern Mediterranean Sea). *Mar Petrol Geol* **26**: 854–872.

Milkov AV (2000) Worldwide distribution of submarine mud volcanoes and associated gas hydrates. *Mar Geol* **167**: 29–42.

Mills HJ, Martinez RJ, Story S & Sobecky PA (2005) Characterization of microbial community structure in Gulf of Mexico gas hydrates: comparative analysis of DNA- and RNA-derived clone libraries. *Appl Environ Microb* **71**: 3235–3247.

Morisita M (1959) Measuring of interspecific association and similarity between communities. *Mem Fac Sci Kyushu Univ Ser E (Biol)* **3**: 65–80.

Nauhaus K, Treude T, Boetius A & Krüger M (2005) Environmental regulation of the anaerobic oxidation of methane: a comparison of ANME-I and ANME-II communities. *Environ Microbiol* **7**: 98–106.

Olu-Le Roy K, Sibuet M, Fiala-M A, Gofas S, Salas C, Mariotti A, Foucher JP & Woodside J (2004) Cold seep communities in the deep eastern Mediterranean Sea: composition, symbiosis and spatial distribution on mud volcanoes. *Deep-Sea Res Pt I* **51**: 1915–1936.

Omoregie EO, Mastalerz V, De Lange G, Straub KL, Kappler A, Røy H, Stadnitskaia A, Foucher JP & Boetius A (2008) Biogeochemistry and community composition of iron- and sulfur-precipitating microbial mats at the Chefren mud volcano (Nile Deep Sea Fan, eastern Mediterranean). *Appl Environ Microb* **74**: 3198–3215.

Omoregie EO, Niemann H, Mastalerz V, de Lange GJ, Stadnitskaia A, Mascle J, Foucher JP & Boetius A (2009) Microbial methane oxidation and sulfate reduction at cold seeps of the deep Eastern Mediterranean Sea. *Mar Geol* **261**: 114–127.

Parkes RJ, Cragg BA, Banning N *et al.* (2007) Biogeochemistry and biodiversity of methane cycling in subsurface marine sediments (Skagerrak, Denmark). *Environ Microbiol* **9**: 1146–1161.

Pedrós-Alió C (2006) Marine microbial diversity: can it be determined? *Trends Microbiol* **14**: 257–263.

Perissoratis C (ed) (2005) *Exploration and Evaluation of the Eastern Mediterranean Gas Hydrates and the Associated Deep Biosphere (Anaximander). Final Report*. Institute of Geology and Mineral Exploration, Athens.

Pernthaler A, Dekas AE, Brown CT, Goffredi SK, Embaye T & Orphan VJ (2008) Diverse syntrophic partnerships from deep-sea methane vents revealed by direct cell capture and metagenomics. *P Natl Acad Sci USA* **105**: 7052–7057.

Pielou EC (1969) Association tests versus homogeneity tests: their use in subdividing quadrats into groups. *Vegetatio* **18**: 4–18.

Ravenschlag K, Sahm K, Pernthaler J & Amann R (1999) High bacterial diversity in permanently cold marine sediments. *Appl Environ Microb* **65**: 3982–3989.

Reed AJ, Lutz RA & Vetriani C (2006) Vertical distribution and diversity of bacteria and archaea in sulfide and methane-rich cold seep sediments located at the base of the Florida Escarpment. *Extremophiles* **10**: 199–211.

Shannon CE & Weaver W (1949) *The Mathematical Theory of Communication*. University of Illinois Press, Urbana, IL.

Spiegelman D, Whissell G & Greer CW (2005) A survey of the methods for the characterization of microbial consortia and communities. *Can J Microbiol* **51**: 355–386.

Tamura K, Dudley J, Nei M & Kumar S (2007) MEGA4: Molecular Evolutionary Genetics Analysis (MEGA) software version 4.0. *Mol Biol Evol* **24**: 1596–1599.

Teske A, Hinrichs KU, Edgcomb V, De Vera Gomez A, Kysela D, Sylva SP, Sogin ML & Jannasch HW (2002) Microbial diversity of hydrothermal sediments in the Guaymas Basin: evidence for anaerobic methanotrophic communities. *Appl Environ Microb* **68**: 1994–2007.

Valentine DL (2007) Adaptations to energy stress dictate the ecology and evolution of the Archaea. *Nat Rev Microbiol* **5**: 316–323.

Webster G, Parkes RJ, Fry JC & Weightman AJ (2004) Widespread occurrence of a novel division of bacteria identified by 16S rRNA gene sequences originally found in deep marine sediments. *Appl Environ Microb* **70**: 5708–5713.

Webster G, John Parkes R, Cragg BA, Newberry CJ, Weightman AJ & Fry JC (2006) Prokaryotic community composition and biogeochemical processes in deep subseafloor sediments from the Peru Margin. *FEMS Microbiol Ecol* **58**: 65–85.

Webster G, Yarram L, Freese E, Köster J, Sass H, Parkes RJ & Weightman AJ (2007) Distribution of candidate division JS1 and other bacteria in tidal sediments of the German Wadden Sea using targeted 16S rRNA gene PCR-DGGE. *FEMS Microbiol Ecol* **62**: 78–89.

Werne JP, Baas M & Sinninghe Damsté JS (2002) Molecular isotopic tracing of carbon flow and trophic relationships in a methane-supported benthic microbial community. *Limnol Oceanogr* **47**: 1694–1701.

Werne JP, Haese RR, Zitter T *et al.* (2004) Life at cold seeps: a synthesis of biogeochemical and ecological data from Kazan mud volcano, eastern Mediterranean Sea. *Chem Geol* **205**: 367–390.

Whittenbury R, Davies SL & Davey JF (1970) Exospores and cysts formed by methane-utilizing bacteria. *J Gen Microbiol* **61**: 219–226.

Wilms R, Koepke B, Sass H, Chang TS, Cypionka H & Engelen B (2006) Deep biosphere-related bacteria within the subsurface of tidal flat sediments. *Environ Microbiol* **8**: 709–719.

Wolda H (1981) Similarity indices, sample size and diversity. *Oecologia* **50**: 296–302.

Woodside JM, Ivanov MK & Limonov AF (1998) Shallow gas and gas hydrates in the Anaximander Mountains region, eastern Mediterranean Sea. *Geol Soc Spec Publ* **137**: 177–193.

Zhang W, Ki J-S & Qian P-Y (2008) Microbial diversity in polluted harbor sediments I: bacterial community assessment based on four clone libraries of 16S rDNA. *Estuar Coast Shelf S* **76**: 668–681.

Zhang Z, Schwartz S, Wagner L & Miller W (2000) A greedy algorithm for aligning DNA sequences. *J Comput Biol* **7**: 203–214.

Supporting Information

Additional Supporting Information may be found in the online version of this article:

Table S1. Archaeal and bacterial 16S rRNA gene phylotypes in the sediment of an active site at the Kazan MV, East Mediterranean Sea.

Please note: Wiley-Blackwell is not responsible for the content or functionality of any supporting materials supplied by the authors. Any queries (other than missing material) should be directed to the corresponding author for the article.

SUPPLEMENTARY MATERIAL

Table S1. Occurring archaeal and bacterial 16S rDNA phylotypes in the sediment of an active site at the Kazan Mud Volcano, East Mediterranean Sea.

Clone	No. of similar clones (>98%)	Putative affiliation	Closest relative description (GenBank accession No.) (similarity)
Archaea			
KZNMV-0-A18	40	ANME2c	fos0626f11 gas hydrate sediment, Hydrate Ridge [AJ890142] (99%)
KZNMV-0-A11	2	ANME3	fos0625e3 gas hydrate sediment, Hydrate Ridge [CR937011] (97%)
KZNMV-0-A40	2	ANME2a,b	fos0642g6 gas hydrate sediment, Hydrate Ridge [CR937012] (99%)
KZNMV-0-A25	1	ANME2c	Eel-36a2A1 methane seep, Eel River Basin [AF354129] (98%)
KZNMV-0-A42	1	ANME3	HydBeg92 methane seep, Hydrate Ridge [AJ578119] (96%)
KZNMV-5-A1	23	ANME-3	fos0625e3 gas hydrate sediment, Hydrate Ridge [CR937011] (98%)
KZNMV-5-A4	12	ANME2a,b	fos0642g6 gas hydrate sediment, Hydrate Ridge [CR937012] (99%)
KZNMV-5-A12	12	Methanosarcinales	GoM161_Arch55 marine sediment, Gulf of Mexico [AM745179] (99%)
KZNMV-5-A10	2	ANME2c	fos0644c1 gas hydrate sediment, Hydrate Ridge [CR937009] (98%)
KZNMV-5-A22	2	MBG D	SBAK-mid-17 marine sediment, Skan Bay [DQ640158] (99%)
KZNMV-5-A8	1	ANME 1	GoM_GC232_4463_Arch67 marine sediment, Gulf of Mexico [AM745239] (96%)
KZNMV-5-A21	1	GoM Arc I	113A33, Chefren MV, Nile fan [EF687612] (99%)
KZNMV-5-A24	1	MBG D	4H11 hydrothermal sediment Guaymas Basin [AY835422] (97%)
KZNMV-5-A46	1	ANME 1	fos0128g3+03e1 microbial mat, Black Sea [CR937008] (98%)

KZNMV-10-A2	21	ANME2a,b	Eel-36a2A4 methane seep, Eel River Basin [AF354128] (98%)
KZNMV-10-A4	12	ANME2c	fos0626f11 gas hydrate sediment from Hydrate Ridge [AJ890142] (99%)
KZNMV-10-A1	11	ANME2a,b	fos0642g6 gas hydrate sediment, Hydrate Ridge [CR937012] (99%)
KZNMV-10-A9	2	MBG B	pMC2A36 hydrothermal vent [AB019720] (92%)
KZNMV-10-A11	1	MBG D	SBAK-mid-17 marine sediment, Skan Bay [DQ640158] (97%)
KZNMV-10-A39	1	MBG D	GoM_GC232_4463_Arch74 marine sediment, Gulf of Mexico [AM745242] (99%)
KZNMV-10-A51	1	ANME3	fos0625e3 gas hydrate sediment from Hydrate Ridge [CR937011] (98%)
KZNMV-25-A6	6	ANME3	fos0625e3 gas hydrate sediment from Hydrate Ridge [CR937011] (97%)
KZNMV-25-A23	20	Methanomicrobiales	4E12 hydrothermal sediment Guaymas Basin [AY835414] (99%)
KZNMV-25-A3	10	ANME 1	GoM_GC232_4463_Arch67 marine sediment, Gulf of Mexico [AM745239] (97%)
KZNMV-25-A11	2	ANME2c	fos0644c1 gas hydrate sediment from Hydrate Ridge [CR937009] (99%)
KZNMV-25-A2	1	MBG D	SBAK-mid-17 marine sediment, Skan Bay [DQ640158] (99%)
KZNMV-25-A18	1	Methanosarcinales	4G12 hydrothermal sediment Guaymas Basin [AY835421] (98%)
KZNMV-25-A19	1	ANME 1	GoM_GC232_4463_Arch67 marine sediment, Gulf of Mexico [AM745239] (96%)
KZNMV-25-A36	1	ANME2a,b	Eel-36a2A4 methane seep, Eel River Basin [AF354128] (99%)
KZNMV-25-A37	1	Guayamas Euryarchaeotal Group	4B09 hydrothermal sediment Guaymas Basin [AY835426] (93%)
KZNMV-25-A58	1	Methanosarcinales	GoM161_Arch55 marine sediment, Gulf of Mexico [AM745179] (99%)
KZNMV-30-A1	16	ANME-3	fos0625e3 gas hydrate sediment from Hydrate Ridge [CR937011] (98%)
KZNMV-30-A8	9	ANME 1	fos0128g3+03e1 microbial mat, Black Sea [CR937008] (99%)

KZNMV-30-A7	8	ANME-2c	fos0626f11 gas hydrate sediment from Hydrate Ridge [AJ890142] (99%)
KZNMV-30-A16	7	ANME2a,b	fos0642g6 gas hydrate sediment, Hydrate Ridge [CR937012] (99%)
KZNMV-30-A14	4	Methanosarcinales	GoM161_Arch55 marine sediment, Gulf of Mexico [AM745179] (99%)
KZNMV-30-A3	2	MBG D	SBAK-mid-17 marine sediment, Skan Bay [DQ640158] (98%)
KZNMV-30-A4	2	ANME 1	fos0128g3+03e1 microbial mat, Black Sea [CR937008] (94%)
Bacteria			
KZNMV-0-B38	6	γ-Proteobacteria	EPR4059-B2-Bc53 ocean crust [EU491555] (98%)
KZNMV-0-B3	4	δ-Proteobacteria	OrigSedB30 Eel River Basin methane seep sediment [FJ264671] (98%)
KZNMV-0-B14	3	γ-Proteobacteria	proteobacterium clone 91 hydrothermal field sediments [FJ205282] (98%)
KZNMV-0-B32	3	ε-Proteobacteria	OrigSed9 Eel River Basin methane seep [FJ264679] (97%)
KZNMV-0-B2	2	γ-Proteobacteria	D2, surface of crab collected from hydrothermal vents in the Pacific-Antarctic Ridge [EU265784] (95%)
KZNMV-0-B4	2	γ-Proteobacteria	LC1133B-37 Lost City Hydrothermal Field [DQ270617] (97%)
KZNMV-0-B8	2	δ-Proteobacteria	Hyd89-22 Cascadia Margin [AJ535247] (98%)
KZNMV-0-B10	2	γ-Proteobacteria	Mn3b-B44 methane seep sediment [FJ264567] (99%)
KZNMV-0-B13	2	Unidentified	CAMV300B902 Gulf of Cadiz [DQ004670] (100%)
KZNMV-0-B15	2	γ-Proteobacteria	LC1133B-37 Lost City Hydrothermal Field [DQ270617] (96%)
KZNMV-0-B18	2	γ-Proteobacteria	JT58-17 cold seep sediment, Japan Trench [AB189342] (95%)
KZNMV-0-B1	1	Planctomycetes	P13-59 Pacific arctic surface sediment [EU287152] (92%)
KZNMV-0-B5	1	γ-Proteobacteria	LC1133B-5 Lost City Hydrothermal Field [DQ270612] (95%)
KZNMV-0-B7	1	δ-Proteobacteria	OalgEIV1-36 endosymbiont of *Olavius agalvensis*

			[AJ620497] (98%)
KZNMV-0-B12	1	Firmicutes	livecontrolB22 Eel River Basin methane seep sediment [FJ264756] (98%)
KZNMV-0-B16	1	WS3	MSB-4E2 mangrove soil [DQ811950] (97%)
KZNMV-0-B19	1	γ-Proteobacteria	048E82 Bering Sea sediment [EU925855] (98%)
KZNMV-0-B21	1	γ-Proteobacteria	152H67 Bering Sea sediment [EU925916] (93%)
KZNMV-0-B23	1	δ-Proteobacteria	GN01-8.004 Hypersaline microbial mat [DQ154844] (92%)
ZNMV-0-B29	1	γ-Proteobacteria	P0X4b3F02 ocean crust [EU491419] (93%)
KZNMV-0-B30	1	JS1	B103G07 marine sediment Santa Barbara Basin [FJ455891] (98%)
KZNMV-0-B33	1	γ-Proteobacteria	LC1446B-37, Lost Hydrothermal City [DQ270629] (96%)
KZNMV-0-B34	1	γ-Proteobacteria	P9X2b7A05 ocean crust [EU491163] (97%)
KZNMV-0-B37	1	δ-Proteobacteria	OT-B17.08 sediment from Okinawa Trough [AB252437] (92%)
KZNMV-0-B39	1	Acidobacteria	MS12-1-H08 hydrothermal vent at Brothers Seamount [AM712325] (95%)
KZNMV-0-B40	1	δ-Proteobacteria	Mn3b-B34 methane seep sediment [FJ264573] (99%)
KZNMV-0-B42	1	Acidobacteria	Belgica2005/10-140-14 marine sediments [DQ351783] (93%)
KZNMV-0-B43	1	γ-Proteobacteria	Mn3b-B36 methane seep sediment [FJ264571] (96%)
KZNMV-0-B44	1	γ-Proteobacteria	CS_B046 Guaymas Basin hydrothermal vent sediment [AF420355] (96%)
KZNMV-0-B47	1	γ-Proteobacteria	C13S-40 Yellow Sea sediment [EU617768] (97%)
KZNMV-0-B49	1	δ-Proteobacteria	B2 epibiotic in crab [EU265788] (96%)
KZNMV-0-B51	1	δ-Proteobacteria	OrigSedB20 Eel River Basin methane seep sediment [FJ264661] (98%)
KZNMV-0-B52	1	δ-Proteobacteria	Amsterdam-2B-43 Amsterdam MV

			[AY592401] (97%)
KZNMV-0-B53	1	WS3	b1bcf1.1.f04.rrna.clone7 [AJ937675] (96%)
KZNMV-0-B54	1	WS3	B78-35 Pacific arctic surface sediment [EU286999] (93%)
KZNMV-0-B55	1	γ-Proteobacteria	OrigSedB29 Eel River Basin methane seep sediment [FJ264669] (96%)
KZNMV-0-B56	1	Bacteriodetes	CK_1C2_44 sediment from Thalassia sea grass bed [EU487946] (93%)
KZNMV-0-B57	1	γ-Proteobacteria	65 EDB1 sediment from oil polluted water [AM882525] (96%)
KZNMV-0-B58	1	Acidobacteria	093B48 Bering Sea sediment [EU734999] (98%)
KZNMV-0-B59	1	γ-Proteobacteria	P13-44 [EU287137] arctic surface sediment (99%)
KZNMV-0-B61	1	WS3	CV39 cave [DQ499291] (91%)
KZNMV-0-B62	1	Bacteriodetes	103G46 Bering Sea sediment [FJ416073] (99%)
KZNMV-0-B63	1	γ-Proteobacteria	Methylobacter_sp. BB5.1 [AF016981] (96%)
KZNMV-0-B64	1	γ-Proteobacteria	Belgica2005/10-120-18 [DQ351749] (91%)
KZNMV-0-B65	1	γ-Proteobacteria	014A22 Bering Sea sediment [EU734923] (98%)
KZNMV-0-B67	1	γ-Proteobacteria	Hyd89-87 Cascadia Margin hydrate sediment [AJ535246] (98%)
KZNMV-0-B68	1	δ-Proteobacteria	A4C hydrothermal field Lau Basin [FJ205191] (92%)
KZNMV-0-B69	1	α-Proteobacteria	LC1133B-64 Lost City Hydrothermal Field [DQ270644] (96%)
KZNMV-0-B70	1	Actinobacteria	S1-16 Yellow Sea sediment [FJ545448] (99%)
KZNMV-5-B4	31	δ-Proteobacteria	hydrocarbon seep sediment Gulf of Cadiz [DQ004674] (99%)
KZNMV-5-B25	9	δ-Proteobacteria	BC-B1_6h Eel River Basin methane seep [EU622291] (99%)
KZNMV-5-B23	8	δ-Proteobacteria	BC_B2_3f Eel River Basin methane seep

			[EU622295] (99%)
KZNMV-5-B3	7	JS1	B103G07 marine sediment Santa Barbara Basin [FJ455891] (97%)
KZNMV-5-B1	2	δ-Proteobacteria	v1t38 tube of a cold seep vestimentiferan [FM165265] (98%)
KZNMV-5-B48	2	δ-Proteobacteria	BC_B2_3f Eel River Basin methane seep [EU622295] (96%)
KZNMV-5-B49	2	unaffiliated	Hyd24-12 Cascadia Margin hydrate sediment [AJ535232] (98%)
KZNMV-5-B64	2	δ-Proteobacteria	BC_B2_4b Eel River Basin methane seep [EU622296] (97%)
KZNMV-5-B10	1	δ-Proteobacteria	Delta V1tb40 [FM165234] (99%)
KZNMV-5-B12	1	Deferribacteres	MD2896-B14 surface sediment China Sea [EU048673] (92%)
KZNMV-5-B16	1	α-Proteobacteria	CM9 Juan de Fuca Ridge [DQ832646] (97%)
KZNMV-5-B17	1	unaffiliated	MD2896-B6 surface sediment China Sea [EU048666] (97%)
KZNMV-5-B20	1	OP8	V1tb47 tube of a cold seep vestimentiferan [FM165244] (94%)
KZNMV-5-B22	1	unaffiliated	CAMV300B915 Gulf of Cadiz seep sediment [DQ004672] (91%)
KZNMV-5-B34	1	δ-Proteobacteria	a2b040 Guaymas Basin hydrate sediment [AF420340] (94%)
KZNMV-5-B40	1	Acidobacteria	113B470 Chefren MV [EF687475] (96%)
KZNMV-5-B42	1	Chloroflexi	CI75cm.2.05 sandy carbonated sediment [EF208701] (93%)
KZNMV-5-B47	1	WS3	CK_1C2_54 sediment from Thalassia sea grass bed [EU487957] (92%)
KZNMV-5-B50	1	Acidobacteria	MS12-1-H08 hydrothermal vent at Brothers Seamount [AM712325] (93%)
KZNMV-5-B55	1	δ-Proteobacteria	Hyd89-04 Hydrate Ridge [AJ535240] (99%)
KZNMV-5-B58	1	OP11	zdt-45e5 [AC160099] (93%)
KZNMV-5-B61	1	δ-Proteobacteria	BC_B2_3f Eel River Basin methane seep

			[EU622295] (96%)
KZNMV-5-B66	1	Defferibacteres	CK_2C6_8 sediment from Thalassia sea grass bed [EU488483] (97%)
KZNMV-5-B67	1	Planctomyces	MSB-2F10 mangrove soil [EF125446] (94%)
KZNMV-5-B68	1	Actinobacteria	VHS-B4-19 harbor sediments [DQ394984] (94%)
KZNMV-5-B70	1	δ-Proteobacteria	Eel-36e1H1 Eel River Basin [AF354164] (96%)
KZNMV-5-B72	1	δ-Proteobacteria	K2-30-4 Lake Kauhako [AY344393] (96%)
KZNMV-5-B76	1	γ-Proteobacteria	D2, surface of crab collected from hydrothermal vents in the Pacific-Antarctic Ridge [EU265784] (97%)
KZNMV-5-B80	1	WS2	071F51 Bering Sea sediment [EU925868] (91%)
KZNMV-5-B83	1	Bacteriodetes	KM66 temperate estuarine mud [AY216454] (96%)
KZNMV-5-B87	1	Planctomycetes	B103B06 marine sediment Santa Barbara Basin [FJ455880] (95%)
KZNMV-5-B89	1	OP8	7_st5_0-2cm Namibian sediment [EU290738] (96%)
KZNMV-5-B92	1	Unidentified	V1tb44 tube of a cold seep vestimentiferan [FM165245] (89%)
KZNMV-5-B94	1	δ-Proteobacteria	so4B2 Eel River Basin methane seep sediment [FJ264777] (92%)
KZNMV-10-B1	9	ε-Proteobacteria	OrigSed9 Eel River Basin methane seep [FJ264679] (98%)
KZNMV-10-B4	4	δ-Proteobacteria	OalgEIV1-36 endosymbiont of *Olavius agalvensis* [AJ620497] (98%)
KZNMV-10-B91	4	γ-Proteobacteria	D2, surface of crab collected from hydrothermal vents in the Pacific-Antarctic Ridge [EU265784] (97%)
KZNMV-10-B8	3	γ-Proteobacteria	S11-46 arctic surface sediment [EU287229] (99%)
KZNMV-10-B13	3	OP8	10bav_H12red continental margin sediments [EU181480] (96%)
KZNMV-10-B27	3	δ-Proteobacteria	OrigSedB20 Eel River Basin methane seep sediment [FJ264661] (98%)
KZNMV-10-B44	3	γ-Proteobacteria	B8S-21 Yellow sea sediment

			[EU652540] (99%)
KZNMV-10-B46	3	δ-Proteobacteria	GoM161_Bac95 Gulf of Mexico [AM745165] (97%)
KZNMV-10-B51	3	α-Proteobacteria	CM9 Juan de Fuca Ridge [DQ832646] (97%)
KZNMV-10-B2	2	JS1	10bav_C6_ARB marine sediment Santa Barbara basin [EU181470] (98%)
KZNMV-10-B22	2	δ-Proteobacteria	Gullfaks_b126 Gullfaks oil and gas fields [FM179902] (98%)
KZNMV-10-B40	2	α-Proteobacteria	HCM3MC80_9F_FL Cretan Margin sediment [EU373863] (97%)
KZNMV-10-B73	2	δ-Proteobacteria	BC_B2_3f Eel River Basin methane seep [EU622295] (99%)
KZNMV-10-B3	1	Deferribacteres	RS06101_B55 cave waters [EU101251] (92%)
KZNMV-10-B5	1	unaffiliated	Hyd24-12 Cascadia Margin hydrate sediment [AJ535232] (98%)
KZNMV-10-B9	1	WS3	CK_2C4_19 sediment from *Thalassia* sea grass bed [EU488308] (95%)
KZNMV-10-B10	1	Firmicutes	EV818BHEB5102502DRLWq27f023 subsurface water, Kalahari Shield [DQ256327] (93%)
KZNMV-10-B11	1	Deferribacteres	MSB-5A6 mangrove soil [DQ811936] (85%)
KZNMV-10-B12	1	OP11	MSB-3A10 mangrove soil [DQ811940] (93%)
KZNMV-10-B14	1	Chloroflexi	CK_1C5_10 sediment from *Thalassia* sea grass bed [EU488103] (97%)
KZNMV-10-B15	1	γ-Proteobacteria	Tomm05_1274_3_Bac27 Tommeliten methane seeps [FM179879] (99%)
KZNMV-10-B17	1	δ-Proteobacteria	Mn3b-B34 methane seep sediment [FJ264573] (99%)
KZNMV-10-B19	1	Acidobacteria	113B470 Chefren MV [EF687475] (98%)
KZNMV-10-B23	1	γ-Proteobacteria	CH2b56 sulfide-microbial incubator [DQ228657] (96%)
KZNMV-10-B26	1	γ-Proteobacteria	CS_B021 Guaymas Basin hydrothermal vent sediment [AF420353] (98%)
KZNMV-10-B32	1	OP11	GoM161_Bac40 Gulf of Mexico

			[AM745145] (93%)
KZNMV-10-B33	1	Acidobacteria	MAT-CR-P5-H06 hypersaline microbial mat [EU246254] (97%)
KZNMV-10-B34	1	Chlorobi	PC06110_B84 cave water [EU101178] [EU246254] (94%)
KZNMV-10-B35	1	Acidobacteria	Sylt 38 Waaden Sea sediment [AM040134] (93%)
KZNMV-10-B38	1	Bacteriodetes	131D74 Bering Sea sediment [EU797471] (99%)
KZNMV-10-B39	1	Acidobacteria	093B48 Bering Sea sediment [EU734999] (98%)
KZNMV-10-B41	1	δ-Proteobacteria	150H57 Bering sea sediment [EU925915] (99%)
KZNMV-10-B45	1	Chloroflexi	CI75cm.2.05 sandy carbonated sediment [EF208701] (90%)
KZNMV-10-B47	1	Chloroflexi	CK_2C6_5 sediment from *Thalassia* sea grass bed [EU488480] (98%)
KZNMV-10-B48	1	Actinobacteria	VHS-B4-19 harbor sediments [DQ394984] (93%)
KZNMV-10-B49	1	δ-Proteobacteria	HMMVBeg-13 Haakon Mosby MV [AJ704676] (91%)
KZNMV-10-B55	1	δ-Proteobacteria	MSB-2E2 mangrove soil [EF125442] (95%)
KZNMV-10-B56	1	Actinobacteria	124D66 Bering sea sediment [EU735028] (98%)
KZNMV-10-B57	1	δ-Proteobacteria	so4B2 Eel River Basin methane seep sediment [FJ264777] (91%)
KZNMV-10-B58	1	Deferribacteres	LCP-26 Saltmarsh clone [AF286031] (93%)
KZNMV-10-B59	1	Planctomycetes	033C34 Bering sea sediment [EU734941] (92%)
KZNMV-10-B61	1	γ-Proteobacteria	032K66 Bering Sea sediment [FJ416087] (97%)
KZNMV-10-B65	1	γ-Proteobacteria	Hyd89-87 Cascadia Margin hydrate sediment [AJ535246] (98%)
KZNMV-10-B66	1	γ-Proteobacteria	Sylt 32 sandy sediment Wadden Sea [AM040128] (99%)
KZNMV-10-B70	1	γ-Proteobacteria	JT58-17 cold seep from Japan Trench

			[AB189342] (96%)
KZNMV-10-B71	1	γ-Proteobacteria	VHS-B1-30 harbour sediments [DQ394903] (94%)
KZNMV-10-B75	1	OP11	GoM161_Bac40 Gulf of Mexico [AM745145] (94%)
KZNMV-10-B76	1	Chloroflexi	CK_1C2_73 sediment from *Thalassia* sea grass bed [EU487978] (92%)
KZNMV-10-B77	1	δ-Proteobacteria	D13S-2 Yellow Sea sediment [EU617833] (97%)
KZNMV-10-B78	1	γ-Proteobacteria	Mn3b-B48 methane seep sediment [FJ264563] (98%)
KZNMV-10-B81	1	δ-Proteobacteria	so4B3 methane seep sediment Cascadian Margin [FJ264783] (97%)
KZNMV-10-B82	1	γ-Proteobacteria	39 EDB1 oil polluted water [AM882526] (93%)
KZNMV-10-B87	1	γ-Proteobacteria	P9X2b3B06 ocean crust [EU491101] (92%)
KZNMV-10-B89	1	Actinobacteria	VHS-B3-77 harbour sediment [DQ394962] (95%)
KZNMV-10-B90	1	γ-Proteobacteria	pItb-vmat-16 microbial mat hot sring [AB294933] (98%)
KZNMV-10-B94	1	δ-Proteobacteria	Tomm05_1274_3_Bac54 Tommeliten methane seeps [FM179884] (99%)
KZNMV-10-B95	1	ε-Proteobacteria	CK_1C2_76 sediment from *Thalassia* sea grass bed [EU487981] (98%)
KZNMV-25-B1	10	Chloroflexi	GoM161_Bac3 Gulf of Mexico [AM745142] (99%)
KZNMV-25-B3	3	γ-Proteobacteria	JT58-17 cold seep from Japan Trench [AB189342] (95%)
KZNMV-25-B8	3	γ-Proteobacteria	LC1133B-37 Lost City Hydrothermal Field [DQ270617] (96%)
KZNMV-25-B11	2	Actinobacteria	D15_10 tar-oil contaminated aquifer sediments [EU266850] (87%)
KZNMV-25-B16	2	Chloroflexi	CI75cm.2.11 sandy carbonated sediment [EF208705] (95%)
KZNMV-25-B49	2	Unidentified	v1t44 tube of a cold seep vestimentiferan [FM165274] (99%)
KZNMV-25-B56	2	γ-Proteobacteria	Hyd89-87 Cascadia Margin hydrate sediment

			[AJ535246] (97%)
KZNMV-25-B4	1	Planctomycetes	HAT5_963 epibiotic in crab [AB476212] (99%)
KZNMV-25-B7	1	γ-Proteobacteria	P13-11 Pacific arctic surface sediment [EU287104] (98%)
KZNMV-25-B10	1	δ-Proteobacteria	Hyd89-22 Cascadia Margin [AJ535247] (98%)
KZNMV-25-B12	1	TG1	D15_17 tar-oil contaminated aquifer sediments [EU266857] (89%)
KZNMV-25-B13	1	γ-Proteobacteria	*Escherichia coli* O157:H7 str. EC4115 [CP001164] (99%)
KZNMV-25-B15	1	ε-Proteobacteria	OrigSed9 Eel River Basin methane seep [FJ264679] (98%)
KZNMV-25-B17	1	γ-Proteobacteria	LC1446B-37 Lost City hydrothermal field [DQ270629] (96%)
KZNMV-25-B19	1	Planctomycetes	P9X2b7A10 ocean crust [EU491166] (91%)
KZNMV-25-B20	1	δ-Proteobacteria	B2 epibiotic in crab [EU265788] (95%)
KZNMV-25-B21	1	ε-Proteobacteria	PB2.9 surface water [DQ071101] (97%)
KZNMV-25-B26	1	JS1	10bav_C6_ARB marine sediment Santa Barbara basin [EU181470] (98%)
KZNMV-25-B29	1	γ-Proteobacteria	JTB35 cold seep sediment Japan Trech [AB015250] (97%)
KZNMV-25-B30	1	γ-Proteobacteria	*Serratia nematodiphila* strain DZ0503SBSH1-2 [EU914257] (99%)
KZNMV-25-B31	1	δ-Proteobacteria	OrigSedB20 Eel River Basin methane seep sediment [FJ264661] (98%)
KZNMV-25-B35	1	Actinobacteria	II10D deep-sea hydrothermal region [FJ205382] (99%)
KZNMV-25-B40	1	δ-Proteobacteria	so4B7 Eel River Basin methane seep sediment [FJ264787] (96%)
KZNMV-25-B41	1	Unidentified	CAMV300B902 hydrocarbon seep sediment Gulf of Cadiz [DQ004670] (99%)
KZNMV-25-B42	1	δ-Proteobacteria	OrigSedB20 Eel River Basin methane seep sediment [FJ264661] (92%)
KZNMV-25-B43	1	δ-Proteobacteria	C13S-128 Yellow Sea sediment

			[EU617741] (98%)
KZNMV-25-B45	1	γ-Proteobacteria	*Acinetobacter johnsonii* [DQ911549] (99%)
KZNMV-25-B46	1	α-Proteobacteria	EPR3970-MO1A-Bc73 ocean crust [EU491659] (98%)
KZNMV-25-B47	1	γ-Proteobacteria	proteobacterium clone 91 hydrothermal field sediments [FJ205282] (98%)
KZNMV-25-B48	1	γ-Proteobacteria	P9X2b3F11 ocean crust [EU491143] (98%)
KZNMV-25-B53	1	γ-Proteobacteria	Endosymbiont of *Bathymodiolus* sp. [AJ745717] (97%)
KZNMV-25-B54	1	δ-Proteobacteria	Amsterdam-2B-43 Amsterdam MV [AY592401] (97%)
KZNMV-25-B55	1	γ-Proteobacteria	OrigSedB28 Eel River Basin methane seep sediment [FJ264668] (96%)
KZNMV-25-B57	1	Deferribacteres	LCP-26 Saltmarsh clone [AF286031] (95%)
KZNMV-25-B58	1	δ-Proteobacteria	AS48 activated sludge from membrane bioreactor [EU283371] (90%)
KZNMV-25-B61	1	α-Proteobacteria	A7C hydrothermal region Lau Basin [FJ205181] (96%)
KZNMV-25-B62	1	Bacteriodetes	131D74 Bering Sea sediment [EU797471] (99%)
KZNMV-25-B65	1	ε-Proteobacteria	BD1-5 deep-sea sediments [AB015518] (91%)
KZNMV-30-B2	24	γ-Proteobacteria	Shigella sp. clone M7-22 [EU530456] (99%)
KZNMV-30-B12	7	Unidentified	CAMV300B902 hydrocarbon seep sediment Gulf of Cadiz [DQ004670] (99%)
KZNMV-30-B6	6	Actinobacteria	D15_10 tar-oil contaminated aquifer sediments [EU266850] (87%)
KZNMV-30-B15	5	Firmicutes	C57 infected cardiac valve [EU557007] (99%)
KZNMV-30-B17	3	α-Proteobacteria	S25_1428 marine microorganisms Coco's Island Costa Rica [EF575084] (99%)
KZNMV-30-B47	3	α-Proteobacteria	*Methylobacterium* sp. iEII3 [AY364020] (99%)
KZNMV-30-B22	2	Firmicutes	E64 deep sea sediment

			[AM085483] (99%)
KZNMV-30-B24	2	JS1	B103G07 marine sediment Santa Barbara Basin [FJ455891] (98%)
KZNMV-30-B31	2	γ-Proteobacteria	P9X2b8G11 ocean crust [EU491318] (98%)
KZNMV-30-B36	2	ε-Proteobacteria	DS094 mangrove [DQ234177] (97%)
KZNMV-30-B39	2	β-Proteobacteria	FGL3_B5 Green Lake [FJ437813] (95%)
KZNMV-30-B70	2	γ-Proteobacteria	Acinetobacter_sp._clone GI5-002-B06 [FJ192980] (99%)
KZNMV-30-B5	1	Firmicutes	EHFS1_S13g clean room environment [EU071516] (99%)
KZNMV-30-B8	1	γ-Proteobacteria	D13S-16 Yellow Sea sediment [EU617749] (94%)
KZNMV-30-B10	1	δ-Proteobacteria	CAMV300B916 hydrocarbon seep sediment Gulf of Cadiz [DQ004674] (99%)
KZNMV-30-B20	1	α-Proteobacteria	KMS200711-181 cropland soil [EU881315] (100%)
KZNMV-30-B30	1	ε-Proteobacteria	CK_1C2_78 sediment from *Thalassia* sea grass bed [EU487983] (97%)
KZNMV-30-B40	1	ε-Proteobacteria	RS06101_B35 cave waters [EU101234] (98%)
KZNMV-30-B41	1	α-Proteobacteria	*Afipia* genosp. 9 strain G8990 [AGU87779] (99%)
KZNMV-30-B44	1	γ-Proteobacteria	y-OTU3 gut flora of *Helicoverpa assulta* [AY758371] (99%)
KZNMV-30-B49	1	Fusobacterium	Fusobacterium sp. clone 180 [EU644478] (99%)
KZNMV-30-B52	1	Acidobacteria	069F42 Bering Sea sediment [EU925866] (93%)
KZNMV-30-B57	1	β-Proteobacteria	Ralstonia metallidurans CH34 [CP000353] (100%)
KZNMV-30-B61	1	Chloroflexi	CK_1C2_19 sediment from *Thalassia* sea grass bed [EU487920] (93%)
KZNMV-30-B62	1	δ-Proteobacteria	OrigSedB20 Eel River Basin methane seep sediment [FJ264661] (98%)
KZNMV-30-B76	1	Firmicutes	GoM_GC232_4463_Bac1 Gulf of Mexico

			[AM745203] (93%)
KZNMV-30-B78	1	β-Proteobacteria	T3_4 PAH-contaminated soil [FJ184338] (99%)

7

8